國 立 交 通 大 學

生物資訊及系統生物研究所

碩 士 論 文

由結構推導蛋白質與蛋白質接觸面的動力學特性

Structure-derived dynamic properties of protein-protein interfaces

研 究 生：林子琳

指導教授：黃鎮剛　教授

中 華 民 國 九十八 年 十二 月

由結構推導蛋白質與蛋白質接觸面的動力學特性

研究生：林子琳　　指導教授：黃鎮剛 教授

國立交通大學

生物資訊及系統生物研究所

摘 要

蛋白質的交互作用完成了許多生物功能。序列研究指出蛋白質與蛋白質作用區富含厭水性胺基酸；然而，目前為止蛋白質的結構資訊尚無法清楚地區分蛋白質與蛋白質的接觸面與其他蛋白質表面。我們在這個研究中分析了兩項與動力學相關的結構資訊：蛋白質與蛋白質接觸面的中心與蛋白質的質心距離比一般蛋白質表面與蛋白質的質心距離小。蛋白質與蛋白質接觸面的中心的加權接觸數目比一般蛋白質表面的加權接觸數目大。這表示蛋白質與蛋白質接觸面的中心是靠近蛋白質的質量中心並且處於擁擠的堆疊狀態。

Structure-derived dynamic properties of protein-protein interfaces

Student: Zih-Lin Lin Advisor: Dr. Jenn-Kang Hwang

National Chiao Tung University

Institute of Bioinformatics and Systems Biology

Abstract

Many biological functions result from the interactions between proteins. From sequence information, studies have revealed that the interaction interfaces are conserved in hydrophobic environments. However, structure information is still not clear enough to differentiate interaction interfaces from protein surfaces. In this study, we analyzed two structural properties related to protein dynamics: the core interface residues are closer to the centroid of protein, and the weighted contact numbers of core interface residues are larger than that of surface residues. The results suggest that the core interface residues are nearness to the protein centroid and in a crowded environment.

誌 謝

謝謝大家!!感恩幫助我完成論文，兩年以來給我支持與鼓勵的所有人!!首先要感謝的是提供我研究機會的黃鎮剛老師，給予我研究上的指教，指點我學術上的迷津，並且鼓勵我以樂觀的想法與不同的角度看待自己的實驗成果。感謝老師讓我了解作研究應有的態度與方法也教導我待人接物的道理。接著我要感謝實驗室研究同仁們：景盛，志豪，志鵬，建華，存操，啟文，彥龍，士中，儼毅，仙蕾，人維對我在程式與實驗設計方面的指導與幫助以及協助我的口試的進行。還有實驗室的研究同仁們：少偉，志杰，肇基，瓊文，松桓，曉芬，乃文，儷芬在我研究生活上的幫忙助益。還要感謝系上朋友們：智先，志偉，慶恩，宗翰，彥修，敬立，廖芹，佳達，昭昉，致宏，在我研究遇到瓶頸時給我的支持與鼓勵。另外，我要特別感謝:志鵬學長，存操學長，啟文學長，士中學長，仙蕾學姊協助我設計實驗也教導我程式邏輯與應用，並且幫助我撰寫論文，教了我實驗低潮時應抱持正面樂觀的態度。我也要感謝我的家人在我背後的支持，還有之義在我旁邊幫我搖旗加油，以及我的愛鼠賈修在新竹陪伴我。紙短情長，再次感謝所有幫助我與陪伴我的人們。

Contents

Introduction

Classifying residues as surface exposed and buried, based on their solvent accessibilities, is a simple but important step towards understanding the contributions of the residues to the structural integrity[1-2]. Surface exposed residues are often crucial for interactions with other proteins and play functional roles while the buried residues contribute more towards stability of the tertiary structures[3]. Proteins perform their function by interacting with other molecules, such as small ligands, lipids, nucleic acids, and other proteins[4]. The recognition of protein-protein interaction sites can be used to identify functionally important amino acid residues, facilitate experimental efforts to catalog protein interactions, enhance computational docking studies and drug designs, as well as enable functional annotation for the growing number of structurally resolved proteins of unknown functions[4].

Identification of the interface between interacting proteins is an important clue to the function of a protein. In general, the problem of recognition of protein–protein interaction sites can be cast as a classification problem, that is, each amino acid residue is assigned to one of two classes: interacting (interfacial) or non-interacting (non-interfacial) residues[4]. The experimental methods such as yeast-two-hybrid screening, immune-precipitation assays and Föster resonance energy transfer (FRET) have been used for detecting whether two proteins interact with each other or not[5-7],

but it is still difficult to use above experimental methods to identify which residues are in the interaction region, called interface. By analyzing the surfaces of proteins, the interfaces can be differentiated from the surfaces of component subunits in protein complexes.

The characteristics of interface residues have been systematically studied. Lo Conte and Chothia *et al.*[8] have analyzed the amino acid compositions of protein-protein complexes. They discovered the interface residues are more aliphatic and aromatic than the rest part of protein surface. Neuvirth *et al.*[9] noticed that polar and hydrophobic residues are more plentiful in the interface than the rest part of surface. Tyr, Met, Cys, and His are favored on binding interface[9]. Zhou and Shan *et al.*[10] observed that the interface residues are apparently more conserved than the non-interfacial surface residues.

The protein dynamics tell us the information about how the protein moves. It is well-known that protein dynamics is highly correlated to protein function. The experimental measurement of the oscillations of an atom around its mean position in a protein structure is called B-factor. The B-factor (also called crystallographic temperature factor and Debye-Waller factor) in protein X-ray structures is an experimental evidence to protein structure dynamics and is closely related to the number of non-covalent neighboring atoms[11]. The Neuvirth *et al.*[9] analyzed the

B-factor of proteins in free form and revealed that the B-factor of interface is slightly lower than that of the surface in the unbound state[9]. This result is consistent with the finding that an interfacial surface region is less flexible than the rest of the protein surface in unbound state[12].

The protein dynamics are usually calculated by mechanical models. Molecular dynamics (MD) simulation is one of the most famous mechanical models used to describe protein flexibility. Molecular dynamics computes the movements of proteins based on bond stretching, bond angle bending, bond twisting, van der Waals and electrostatic interaction[13-15]. The main drawback of MD simulation is its high computational cost[16-17]. Several prediction methods for protein dynamics elaborated based on protein structures overcame this limitation. For example, the centroid model (CM)[18] and weighted contact number model (WCN)[19] developed by our group. The CM computes protein dynamics directly from the protein geometrical shape. The CM method is based on the observation that the deeper an atom is buried inside a protein structure, the less it will fluctuate around its equilibrium position[18]. The CM only computes the coordinates of Cα atoms and plainly defines the center of mass of a protein. The distance square between the Cα atoms to the center of mass of the protein is accordant to the thermal fluctuation. The atomic fluctuation is in fact linearly related to the square of the atomic distance from the center of mass of the

protein[18]. The weighted contact number model (WCN) calculates the number of neighbor atoms which is weighted by inverse distance between two atoms of each pair. The WCN computes protein dynamics from the protein packing. If an atom is more crowded in a protein structure, the less it will fluctuate around its equilibrium position[19]. We use the CM and WCN to analysis the differences between interfaces and the rest part of the surfaces. We applied the two methods to protein-protein complexes and found the correlation between protein dynamics and interface residues. In the work presented here, the distance to the protein centroid and the weighted contact number were analyzed for both interfaces and surfaces. These two structural properties may give new sights on the comprehension of protein-protein interactions.

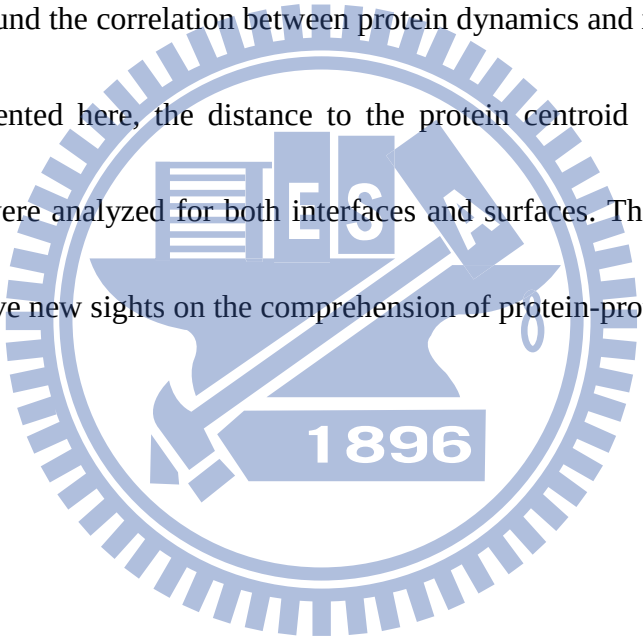

Materials and Methods

We use the ProMate database and ZW databases to analyze the components of protein interface residues and surface residues. And we have further defined the interface residues as core interface residues and peripheral interface residues. Core interface develops the center region of interface and peripheral interface contrasts the rim area of interface. The core interface and peripheral interface together form the interface. We analysis the components and tendencies of core interface and peripheral interface.

ProMate database

ProMate database[9] contains 57 protein-protein interaction structures. The database consists of both the unbound and bound states for transient protein-protein hetero-dimers derived from the PDB[20]. The unbound and bound states of proteins were determined by X-ray crystallography or NMR. The ProMate database has 42 X-ray structures protein structures in unbound form.

The ProMate database was extracted from a database of 92 bound monomers longer than 85 AA. The combinatorial extension method (CE)[21] was prosecuted to find each possible pair of monomers and one of them would be executed from ProMate dataset. The highest sequence identity according to CE is 19.3%.

The unbound structures were then derived from the bound structures. 57 monomers in bound form were found to have a highly homologous unbound form in the PDB[20] by using BLAST[22], with more than 70% sequence identity.

ZW database

The ZW dataset contains 101 transient protein-protein complexes. The 101 transient protein-protein complexes were retrieved from the Zhiping Weng's transient databases[23]. The Zhiping Weng group had collected 212 non-redundant transient hetero-dimeric X-ray structures of protein-protein interactions[24].

To obtain data for hetero-dimers, the Zhiping Weng group only kept the records of X-ray structures better than 3.25 Å and all the chains in the database are longer than 25 amino acids. They eliminated all homomeric records using the BLASTCLUST algorithm[25]. A homomeric record was defined which all chains have 85% sequence identity to each other and at least 50% of the sequence was aligned. To receive a non-redundant database of protein complexes, they used pairwise BLAST[22] to check each pair of all chains in the database and deleted one complex of the pair with 25% sequence identity.

And we have further used global sequence alignment to check each pair of each chain in the database and removed one complex of the pair with 25% sequence

identity. We remained 101 transient protein-protein complexes in the ZW database.

Surface and interface definition

We took the bound state complexes apart and treated the subunits as the unbound state of complexes. After clarifying the corresponding residues between unbound state and bound state for protein-protein complexes, we explored the surface residues and interface residues.

The accessibility(%) plays an important role in definition of surface and interface. Accessibility(%) is presented as

$$Accessibility_i(\%) = \frac{SA_i}{Standard\ \ SA_i} 100\% \quad (1)$$

Accessibility(%) of the *i*-th residue, $Accessibility_i(\%)$, is defined as the ratio of the solvent exposed surface area of the *i*-th residue. SA_i is the solvent exposed surface area of the *i*-th residue and *Standard* SA_i is the standard value of the solvent exposed surface area for this kind of amino acid[26]. We use the DSSP program[27] to calculate exposed surface areas in unbound state and bound state of protein-protein complexes. We defined the surface residue based on the accessibility(%) in unbound state and the interface residue based on the delta accessibility(%) upon complex formation[28]. A residue was categorized as a surface residue if its accessibility(%) in free form is larger than 0. An interface residue is defined as the residue having lost accessibility(%)

upon complex formation. And we further separated interfaces as core interfaces and peripheral interfaces based on the accessibilities(%) in bound state. If an interface residue has the accessibility(%) in the complex smaller than or equal to 5, it is a core interface residue, else it is a peripheral interface residue. An interface residue is taken as either a core interface residue or a peripheral interface residue. The definition of surface, interface, core interface and peripheral interface are showed in Figure 1~Figure 3, and one example is pictured in Figure 4.

Amino acid components

We have calculated the amino acid propensities using the following equations:

$$Propensity_{Target} = \frac{Occurence_{Target}}{Occurence_{Surface}} \quad (2)$$

Where $Propensity_{Target}$ is the amino acid type propensity of the target residues. $Occurence_{Target}$, $Occurence_{Surface}$ are the amino acid type occurrences of the target residues and the surface residues.

Secondary structure definition

The secondary structure is defined by DSSP[27] program. DSSP recognizes eight types of secondary structure, depending on the pattern of hydrogen bonds and 3D protein structures. The eight classes of secondary structures are defined in DSSP:

H: α-helix

B: residue in isolated β-bridge

E: extended strand, participates in β ladder

G: 3/10 helix

I: π-helix

T: hydrogen bonded turn

S: bend

U: undefined

These eight types are usually grouped into three larger classes: helix (G,H, and I), strand (E and B), and loop (all others).

Centroid Model (CM)

Let X_0 be the center of mass of the protein, which is express as

$$X_0 = \sum_k m_k X_k / \sum_k m_k \quad (3)$$

Where m_k and X_k are the mass and the crystallographic position of Cα atom k, respectively. The distance of the Cα atom i from the center of mass of the protein is expressed as

$$r_i^2 = (X_i - X_0)(X_i - X_0) \quad (4)$$

Where Xi and X_0 are the center of mass of the Cα atom i and the protein. Each protein

of size N has the square distance of each Cα atom given by $(r_1^2, r_2^2, \ldots, r_n^2)$. The r^2 profile is closely related to the thermal B-factor, which is given as

$$B_i = (\frac{8\pi^2}{3})(\delta X_i \delta X_i) \quad (5)$$

The centroid model suggest the following interesting relation,

$$\langle \delta X_i \delta X_i \rangle \sim (X_i - X_0)(X_i - X_0) \quad (6)$$

And equation (5) and (6) suggests that the fluctuation of a residue is usually proportional to the distance between center of mass and its position.

Weighted Contact-Number model (WCN)

When the neighboring contact number of an atom is larger, the fluctuation of the atom will be smaller. We can define WCN model as

$$V_i = \sum_{j \neq i}^{N} (1/{r_{ij}}^2) \quad (7)$$

The equation (7) defines V_i, the number of Cα atoms which surround the i^{th} residue. The influence of atom j to the atom i is attenuated by the factor ${1/r_{ij}}^2$. r_{ij} is the distance between Cα atoms of residues *i* and *j*.

Z-score

On the mission to compare the results, we would normalize the ${r_i}^2$ of CM and V_i of WCN to z-scores as

$$z_{x_i} = (x_i - \bar{x})/\sigma_x \quad (8)$$

$\bar{x}$ is the mean of *x* and is the standard deviation of *x*, where the x_i represents the r_i^2 of CM and v_i of WCN.

Two-sample *t*-test

To compare the differences between interfaces and the rest part of the surfaces, we use the two-sample *t*-test.

$$t = \frac{\bar{x} - \bar{y}}{\sqrt{\frac{s_x^2}{m} + \frac{s_y^2}{n}}} \quad (9)$$

Where $\bar{x}$ and $\bar{y}$ are the sample means, s_x and s_y are the sample standard deviations, and *m* and *n* are the sample sizes of the two groups. When a *t* is determined, a *p*-value could be decided from the Student's *t*-distribution table. If the *p*-value is lower than 0.05, the two sample have differences.

Results and Discussions

Amino acid components

The amino acid distributions of core interfaces, peripheral interfaces and interfaces could give a general indication of relative importance of different amino acids. Percentage frequencies and propensities of amino acids were calculated for each amino acid type and the results were illustrated in Figure 5~10.

Cys, Trp, His, Met, Ile are the most dominant amino acid types in the core interface in the ProMate database and Cys, Trp, Phe, Tyr, and Leu are the most abundant amino acids in the core interface in the ZW dataset. Arg, Asp, Glu, Gln, and Asn are the most dominant amino acids in the peripheral interfaces in the ProMate database. Arg, Glu, Lys, His and Glu are the most dominant amino acids in the peripheral interfaces in the ZW database. We could observed that the core interface prefers polar, uncharged and aromatic amino acids whereas the peripheral interface likes charged residues.

Secondary structure constituents

The occurrences of secondary structures are represented in Figure 11~13. The rigid secondary structures, helices and strands, are preferred in the core interfaces compared with surfaces and the flexible secondary structures, loops, are unfavorable

in the core interfaces contract to surfaces. The flexible secondary structures, loops, are preferred in the peripheral interfaces compared with surfaces and the rigid secondary structures, helices and strands, are unfavorable in the peripheral interfaces contract to surfaces.

Accessibilities and delta accessibilities

The accessibility distributions in unbound state are pictured in Figure 14~16. The accessibilities of core interfaces are lower than that of surfaces and the accessibilities of peripheral interfaces are higher than that of surfaces. The analysis of accessibilities revealed that the peripheral interfaces are significantly more accessible than the rest of surfaces.

The delta accessibilities in complexation are pictured in Figure 17~18. There is no difference of delta accessibility distributions between core interfaces, peripheral interfaces, and interfaces.

Evolutionary conservation

It is interesting to research the conservation degree of proteins if the protein-protein interactions play important part in function. We measured the conservation grades using the ConSurf database[29]. The conservation score of a residue

corresponds to its evolutionary rate. The residues evolve slowly are directed to be conserved residues. The lower the conservation score obtained from ConSurf, the higher the conservation degree the residue has.

We could see that the conservation scores are much lower in the core interfaces in Figure 19. The *p*-values between core interfaces and surfaces in the ProMate database and the ZW database are both 0.00. Figure 20 represents that there is no difference between the conservation scores of peripheral interface and surface. The *p*-values between peripheral interfaces and surfaces in the ProMate database and the ZW database are 2.39×10^{-2}, and 5.30×10^{-3} sequentially. Figure 21 shows the tendencies of conservation scores of interface and surfaces. We could see that the conservation scores are lower in the interfaces than that in the surfaces. The *p*-values of conservation scores of the ProMate database, the ZW database are 1.33×10^{-5}, 1.66×10^{-11} sequentially. The analysis of conservation scores revealed that the core interfaces play important roles in protein-protein interactions and the core interfaces are more conserved than the rest part of surfaces.

B-factors

The X-ray crystallization structures from Protein Data Bank offer the B-factor information for each residue in proteins. The B-factors are the oscillations gained by

experiments and related to protein structure dynamics. The higher the B-factor the residue has, the more flexible the residue is.

We analyzed the B-factor distributions in unbound form of the ProMate database. We used the EMBOSS Pairwise Alignment Algorithm[30] to search for regions of local similarity and homologous residues between the two sequences of unbound state and bound state for protein-protein complexes. We found that the B-factors in unbound form of core interfaces are significantly lower than that of surfaces (Figure 22) and the *t*-test comparing core interfaces and surfaces gave a *p*-value of 1.07×10^{-10}. The B-factors in unbound form of peripheral interfaces are slightly higher than that of surfaces (Figure 23) and the *p*-value is 1.31×10^{-10}. The B-factors of interfaces have no difference with that of surfaces (Figure 24) and the *p*-value is 3.97×10^{-2}. We could notice greatly dissimilarity between core interface and surfaces. We could observed from the B-factor presences that the core interfaces are more rigid than the surfaces and the peripheral interfaces are slightly elastic than the surfaces in unbound state.

Figure 31 depicts the protein structure of pdbid 1tmq. We could exam the B-factors of core interface and peripheral interfaces of the chain A of 1tmq in the upper figure. The B-factors of 1tmqA were obtained from the homologous protein of 1tmqA, 1jae_. The red color represents high B-factor values and the blue color

expresses low B-factor values respectively. We could contract the upper and lower figures and perceive that the B-factors of core interfaces are much lower than that of the rest of the surfaces.

Centroid Model (CM)

The centroid model (CM) only computes the distance square between each Cα atom to the center of mass of the protein. The CM method is based on the observation that the deeper an atom is buried inside a protein structure, the less it will fluctuate around its equilibrium position.

We measured the CM distributions of protein-protein interactions in unbound state. The CM of the core interfaces is significantly lower than the CM of the surfaces in unbound form (Figure 25) and the *p*-values of ProMate database, ZW database both are 0.00. The CM of the peripheral interfaces is lightly higher than the CM of the surfaces in unbound form (Figure 26) and the *p*-values of ProMate database, ZW database are 2.77×10^{-6}, and 0.00. The CM distributions have no significant difference between the interfaces and the surfaces (Figure 27). The two sample *t*-test gave *p*-values between the interfaces and surfaces of the two databases with 3.16×10^{-1}, 2.70×10^{-4}. The core interfaces are close to the center of mass of protein structures in the unbound state. The distances between peripheral interfaces and the

center of mass of protein structures are slightly longer than that between surfaces and the center of mass of protein structures.

Visualization of the example of CM model was described in Figure 32. The average distance between surfaces and the center of mass of 1tmqA is 22.62 Å. The distance between the core interface residue, W56, and the center of mass is 16.79 Å. The distance between the peripheral interface residue, E229, and the center of mass is 24.62 Å. The distances of the core interfaces are shorter than that of the surfaces.

Weighted Contact Number model (WCN)

The weighted contact number model (WCN) estimates protein dynamics by calculating the protein packing denseness. The WCN model computes the number of neighboring atoms which is weighted by inverse distance between two atoms of each pair. The WCN is based on that the more crowded an atom is around its environment in a protein structure, the less it will swing around its equilibrium position.

Examining Figure 28 reveals that core interfaces have much higher WCN than the whole surfaces. The two sample *t*-test contrast the core interfaces and the whole surfaces and gave both *p*-values of 0.00 in the ProMate database and the ZW database. Figure 29 shows that peripheral interfaces have much lower WCN than the whole surfaces. The two sample *t*-test contrast the peripheral interfaces and the whole

surfaces and gave both *p*-values of 0.00 in the ProMate database and the ZW database. Observing Figure 30 reveals that the interfaces have lower WCN than the whole surfaces. The two sample *t*-test contrast the interfaces and the whole surfaces and gave *p*-values of 7.54×10^{-13}, 0.00 individually in the ProMate database, the ZW database. The core interfaces have high packing densities and the peripheral interfaces have low packing densities in unbound state.

We could also observe from Figure 33 that the core interfaces are sunken on the surface and the peripheral interfaces are protruding on the surface. The example of Figure 33 agrees with the results of WCN model. It shows that core interface is in a crowded environment and the peripheral interface is not.

Summary

The results of B-factors, WCN, CM suggest that the core interfaces are rigid and the peripheral interfaces are plastic on the surface. The analysis of protein secondary structures also supports the dynamic observations. The evolutionary conservation measurements exposed that the core interfaces are more conserved in the surface whereas the peripheral interfaces are not. It means the core interfaces play important role in protein-protein interactions.

By observing the tendencies of core interfaces, we revealed the important sites in

protein-protein interaction are rigid. And we could further use these structure tendencies to predict protein-protein interfaces in the future.

References

1. Pollastri G, Baldi P, Fariselli P, Casadio R. Prediction of coordination number and relative solvent accessibility in proteins. Proteins 2002;47(2):142-153.
2. Rost B, Sander C. Conservation and prediction of solvent accessibility in protein families. Proteins 1994;20(3):216-226.
3. Chan HS, Dill KA. Origins of structure in globular proteins. Proc Natl Acad Sci U S A 1990;87(16):6388-6392.
4. Porollo A, Meller J. Prediction-based fingerprints of protein-protein interactions. Proteins 2007;66(3):630-645.
5. Young KH. Yeast two-hybrid: so many interactions, (in) so little time. Biol Reprod 1998;58(2):302-311.
6. Crowell RE, Du Clos TW, Montoya G, Heaphy E, Mold C. C-reactive protein receptors on the human monocytic cell line U-937. Evidence for additional binding to Fc gamma RI. J Immunol 1991;147(10):3445-3451.
7. Jares-Erijman EA, Jovin TM. FRET imaging. Nat Biotechnol 2003;21(11):1387-1395.
8. Lo Conte L, Chothia C, Janin J. The atomic structure of protein-protein recognition sites. J Mol Biol 1999;285(5):2177-2198.
9. Neuvirth H, Raz R, Schreiber G. ProMate: a structure based prediction program to identify the location of protein-protein binding sites. J Mol Biol 2004;338(1):181-199.
10. Zhou HX, Shan Y. Prediction of protein interaction sites from sequence profile and residue neighbor list. Proteins 2001;44(3):336-343.
11. Halle B. Flexibility and packing in proteins. Proc Natl Acad Sci U S A 2002;99(3):1274-1279.
12. Jones S, Thornton JM. Protein-protein interactions: a review of protein dimer structures. Prog Biophys Mol Biol 1995;63(1):31-65.
13. Levitt M, Warshel A. Computer simulation of protein folding. Nature 1975;253(5494):694-698.
14. Warshel A. Bicycle-pedal model for the first step in the vision process. Nature 1976;260(5553):679-683.
15. McCammon JA, Gelin BR, Karplus M. Dynamics of folded proteins. Nature 1977;267(5612):585-590.
16. Pandey BP, Zhang C, Yuan X, Zi J, Zhou Y. Protein flexibility prediction by an all-atom mean-field statistical theory. Protein Sci 2005;14(7):1772-1777.
17. Rueda M, Ferrer-Costa C, Meyer T, Perez A, Camps J, Hospital A, Gelpi JL, Orozco M. A consensus view of protein dynamics. Proc Natl Acad Sci U S A

2007;104(3):796-801.
18. Shih CH, Huang SW, Yen SC, Lai YL, Yu SH, Hwang JK. A simple way to compute protein dynamics without a mechanical model. Proteins 2007;68(1):34-38.
19. Lin CP, Huang SW, Lai YL, Yen SC, Shih CH, Lu CH, Huang CC, Hwang JK. Deriving protein dynamical properties from weighted protein contact number. Proteins 2008;72(3):929-935.
20. Berman HM, Westbrook J, Feng Z, Gilliland G, Bhat TN, Weissig H, Shindyalov IN, Bourne PE. The Protein Data Bank. Nucleic Acids Res 2000;28(1):235-242.
21. Shindyalov IN, Bourne PE. Protein structure alignment by incremental combinatorial extension (CE) of the optimal path. Protein Eng 1998;11(9):739-747.
22. Altschul SF, Madden TL, Schaffer AA, Zhang J, Zhang Z, Miller W, Lipman DJ. Gapped BLAST and PSI-BLAST: a new generation of protein database search programs. Nucleic Acids Res 1997;25(17):3389-3402.
23. Mintseris J, Weng Z. Structure, function, and evolution of transient and obligate protein-protein interactions. Proc Natl Acad Sci U S A 2005;102(31):10930-10935.
24. Mintseris J, Weng Z. Atomic contact vectors in protein-protein recognition. Proteins 2003;53(3):629-639.
25. Johnson M, Zaretskaya I, Raytselis Y, Merezhuk Y, McGinnis S, Madden TL. NCBI BLAST: a better web interface. Nucleic Acids Res 2008;36(Web Server issue):W5-9.
26. Rose GD, Geselowitz AR, Lesser GJ, Lee RH, Zehfus MH. Hydrophobicity of amino acid residues in globular proteins. Science 1985;229(4716):834-838.
27. Kabsch W, Sander C. Dictionary of protein secondary structure: pattern recognition of hydrogen-bonded and geometrical features. Biopolymers 1983;22(12):2577-2637.
28. Jones S, Thornton JM. Analysis of protein-protein interaction sites using surface patches. J Mol Biol 1997;272(1):121-132.
29. Landau M, Mayrose I, Rosenberg Y, Glaser F, Martz E, Pupko T, Ben-Tal N. ConSurf 2005: the projection of evolutionary conservation scores of residues on protein structures. Nucleic Acids Res 2005;33(Web Server issue):W299-302.
30. Smith TF, Waterman MS. Identification of common molecular subsequences. J Mol Biol 1981;147(1):195-197.

Figures

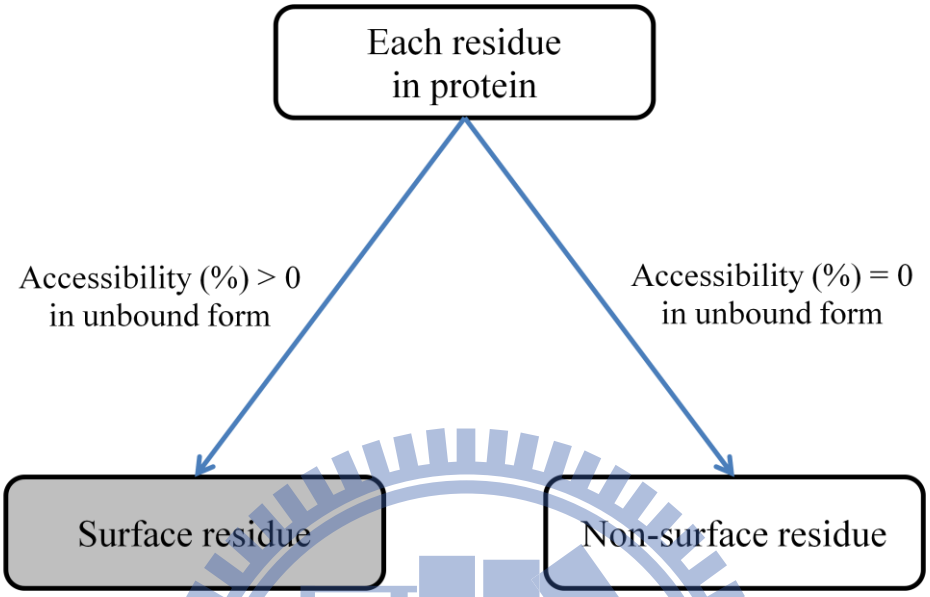

Figure 1. The definitions of surface and non-surface.

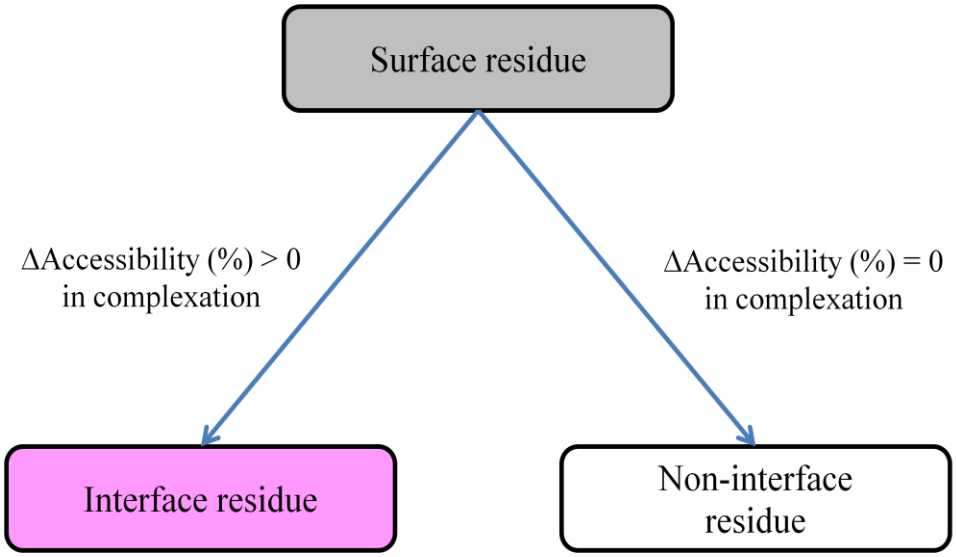

Figure 2. The definitions of interface and non-interface.

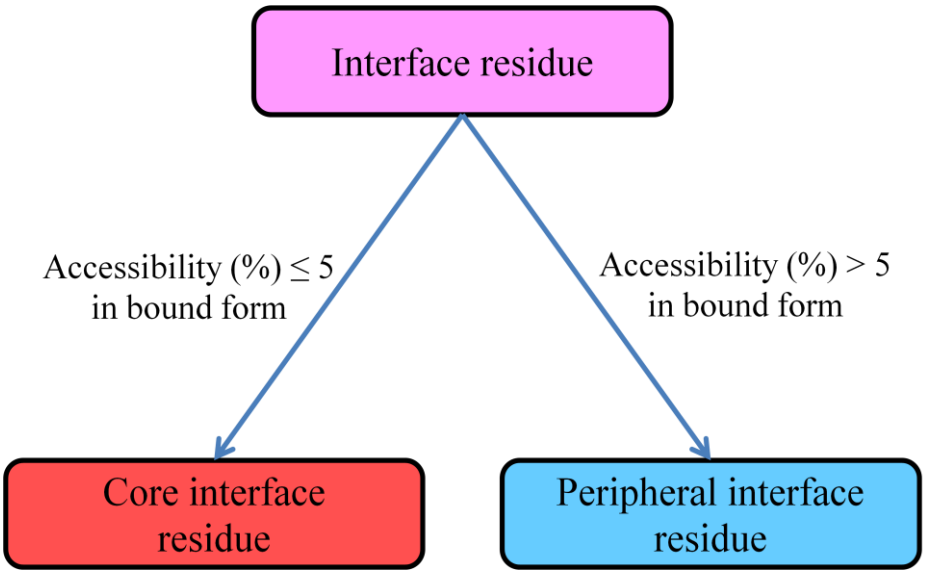

Figure 3. The definitions of core interface and peripheral interface.

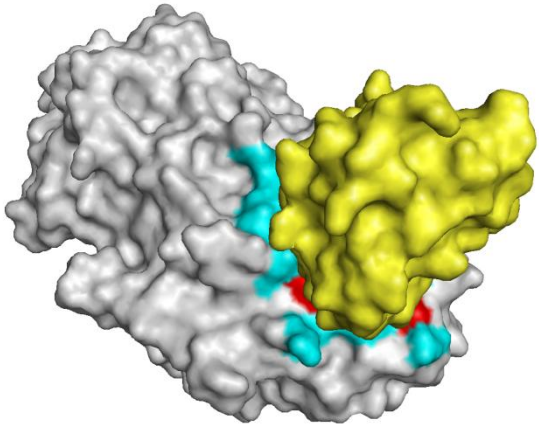

(A)

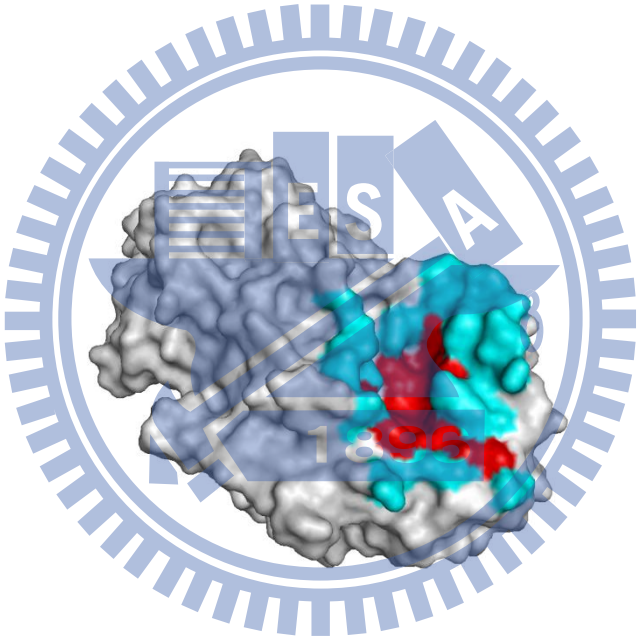

(B)

Figure 4. Visualization of the core interface and the peripheral interface (PDB entry 1tmq) (A) Chain A and chain B. (B) Chain A only. Visual graphics tool Pymol was used to visualize the core interface and peripheral interface of 1tmqA. The chain A was shown in gray and chain B was shown in yellow. The core interface and the peripheral interface of chain A were emphasized in red and cyan independently.

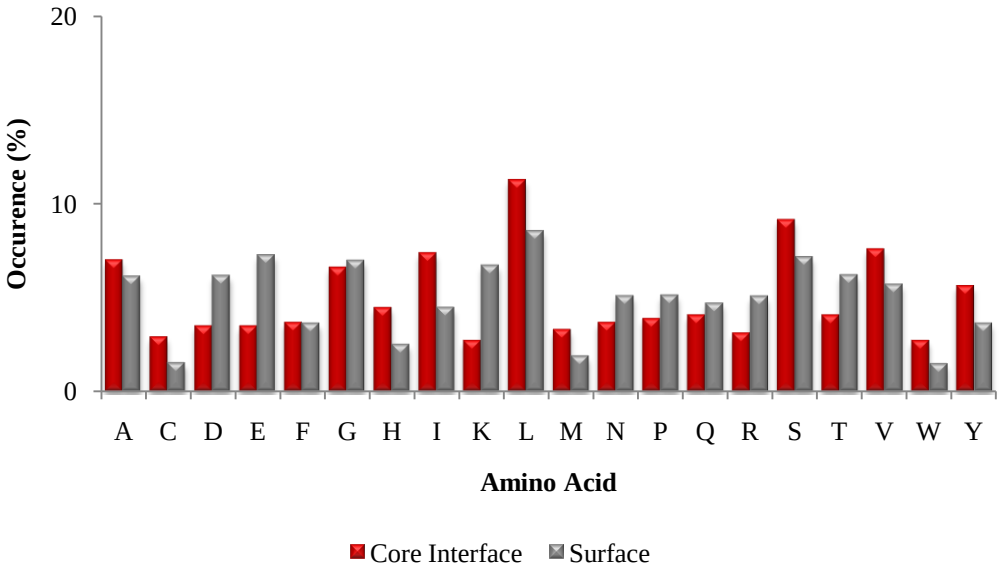

(A)

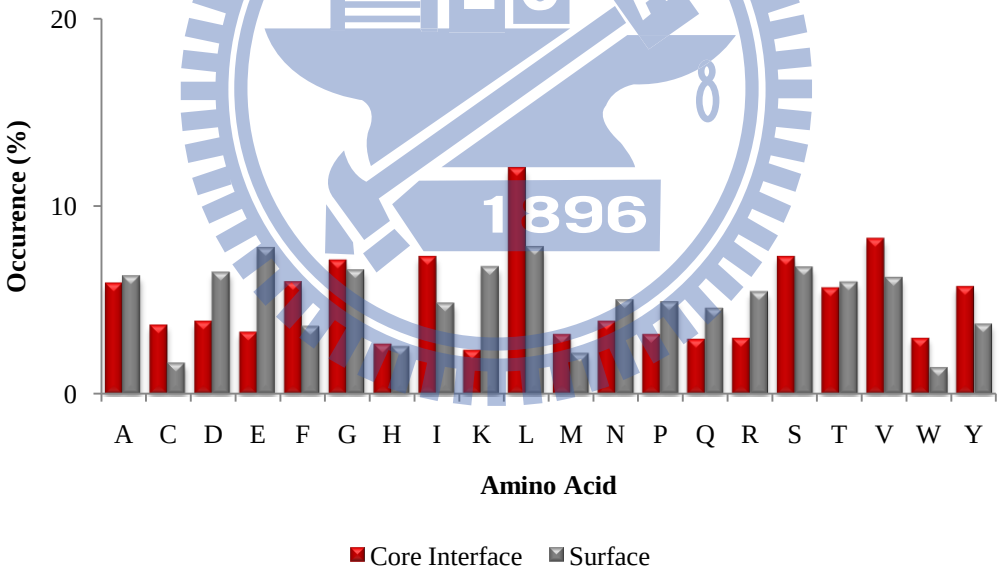

(B)

Figure 5. Comparison of the amino acid distributions between core interfaces and surfaces in unbound state of (A) the ProMate database (B) the ZW database.

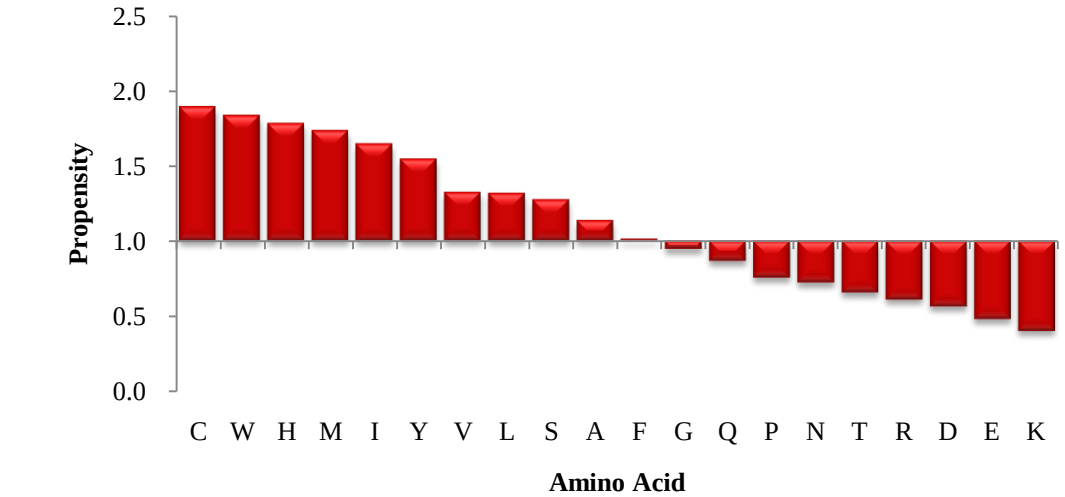

(A)

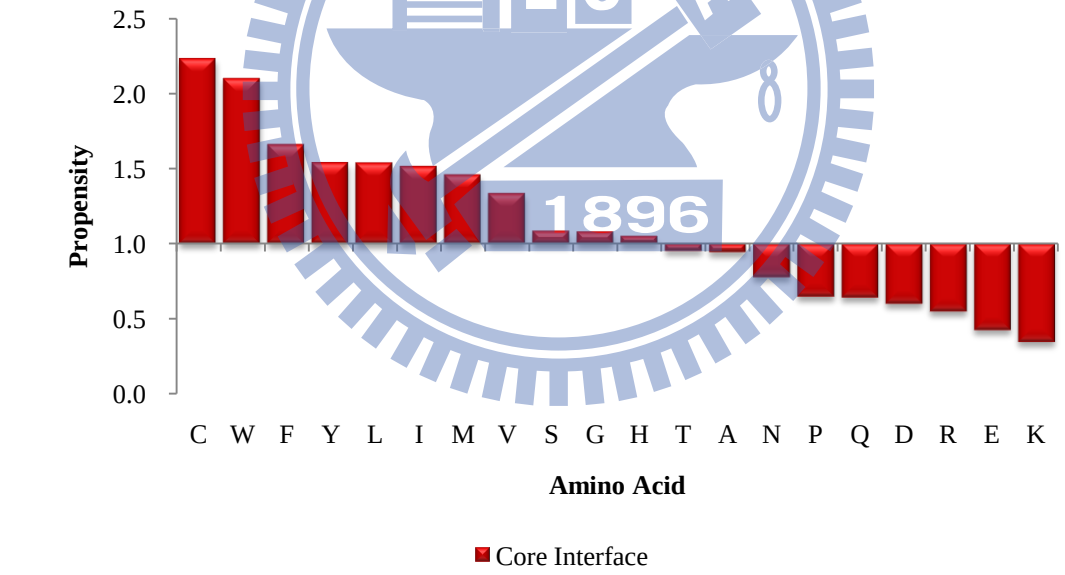

(B)

Figure 6. The amino acid propensities of core interfaces in unbound state of (A) the ProMate database (B) the ZW database.

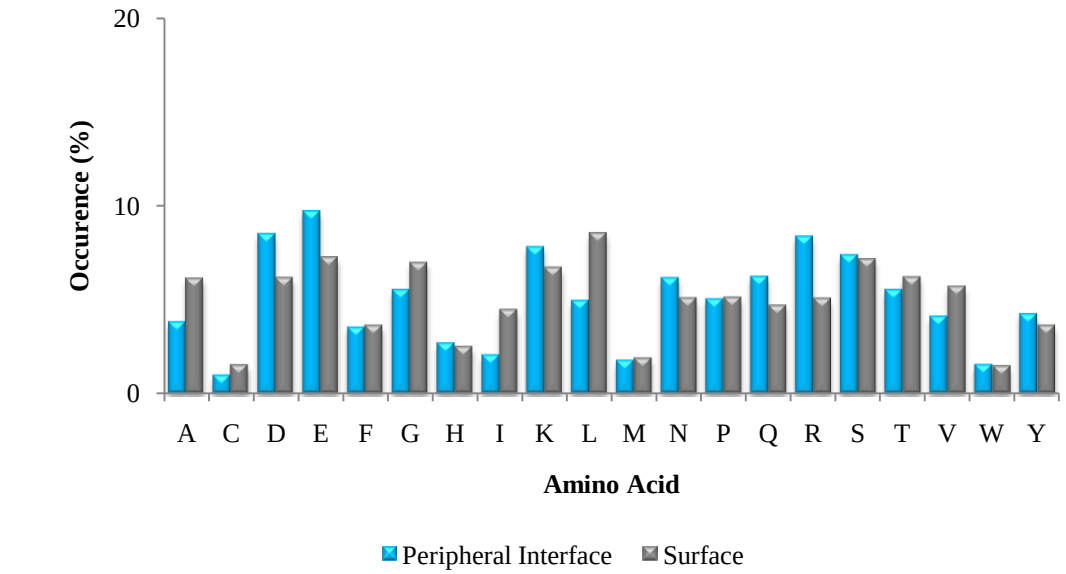

(A)

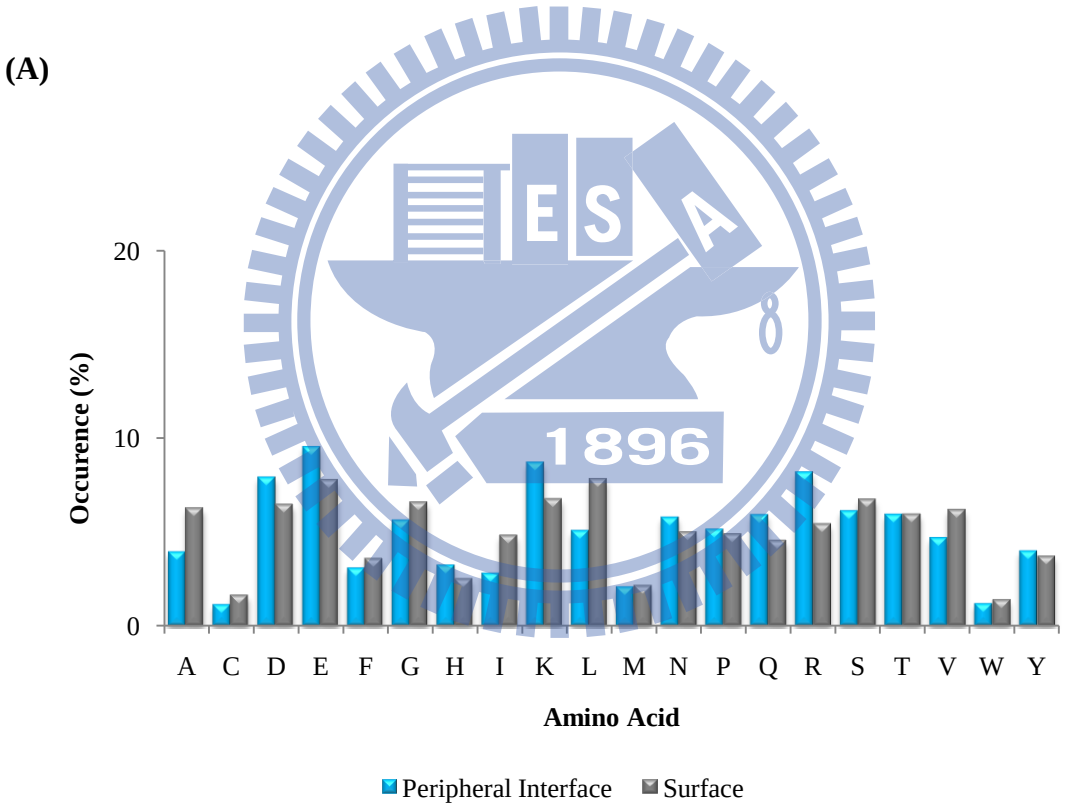

(B)

Figure 7. Comparison of the amino acid distributions between peripheral interfaces and surfaces in unbound state of (A) the ProMate database (B) the ZW database.

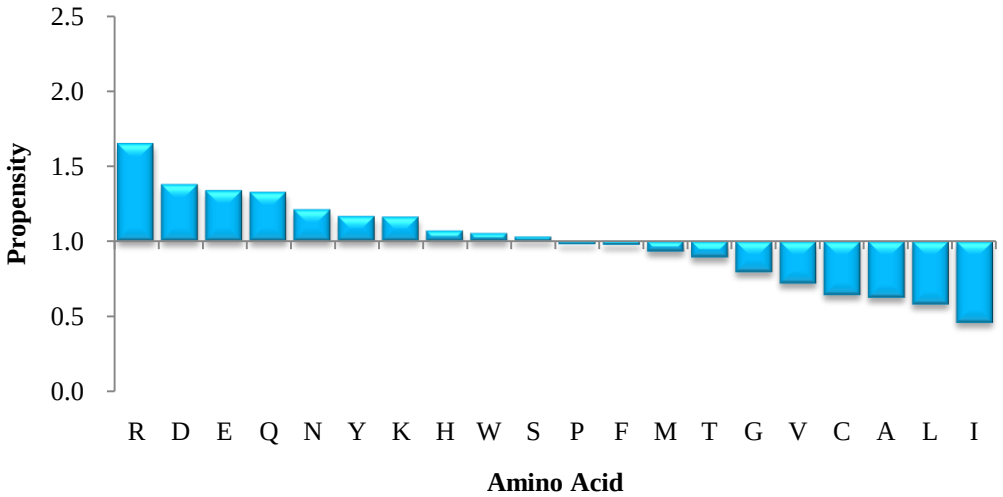

(A)

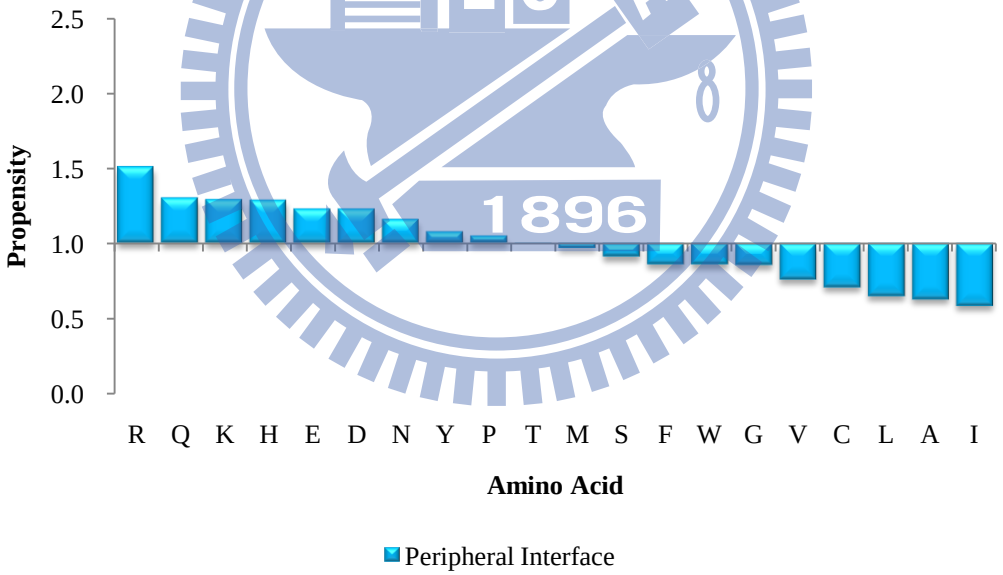

(B)

Figure 8. The amino acid propensities of peripheral interfaces in unbound state of (A) the ProMate database (B) the ZW database.

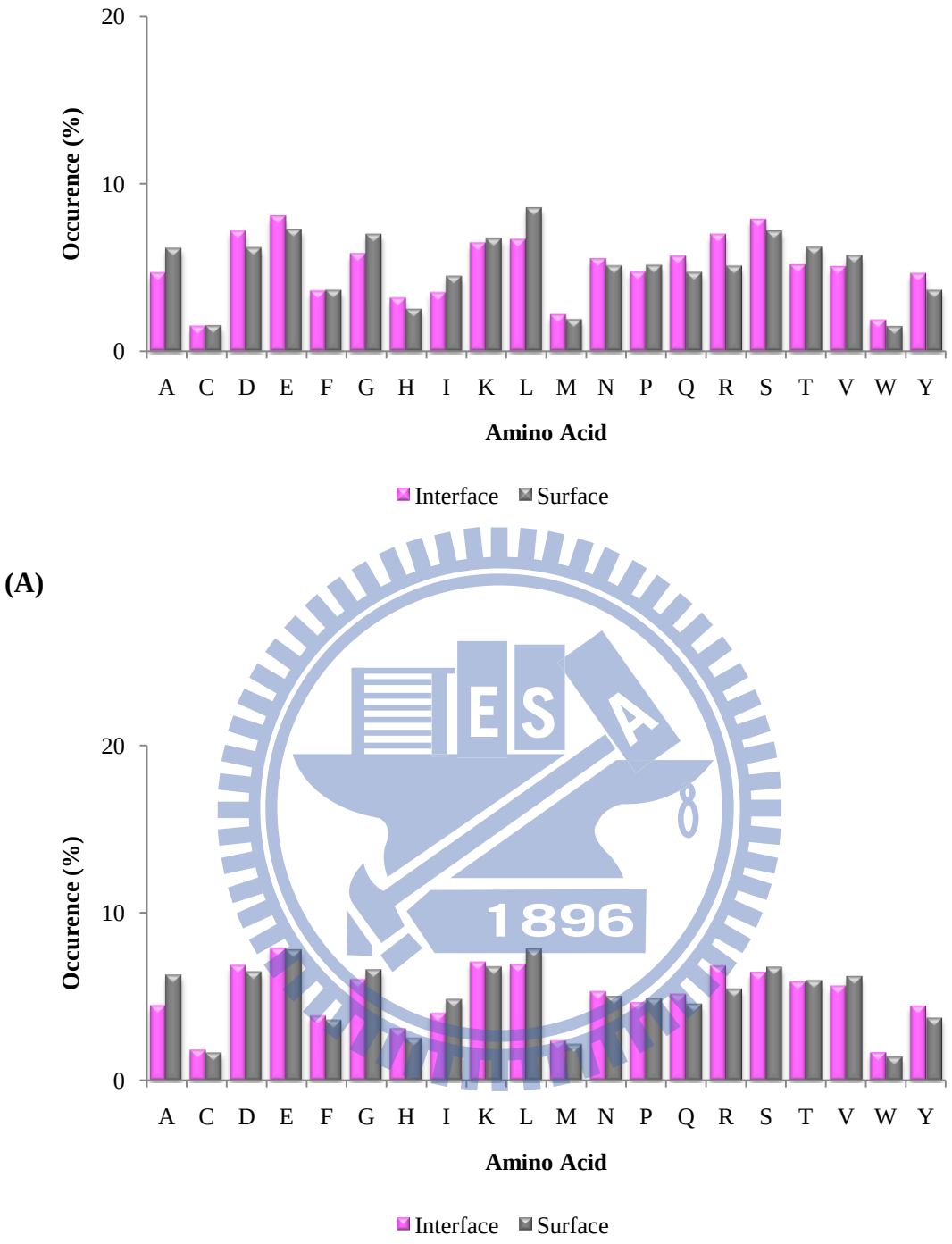

Figure 9. Comparison of the amino acid distributions between interfaces and surfaces in unbound state of (A) the ProMate database (B) the ZW database.

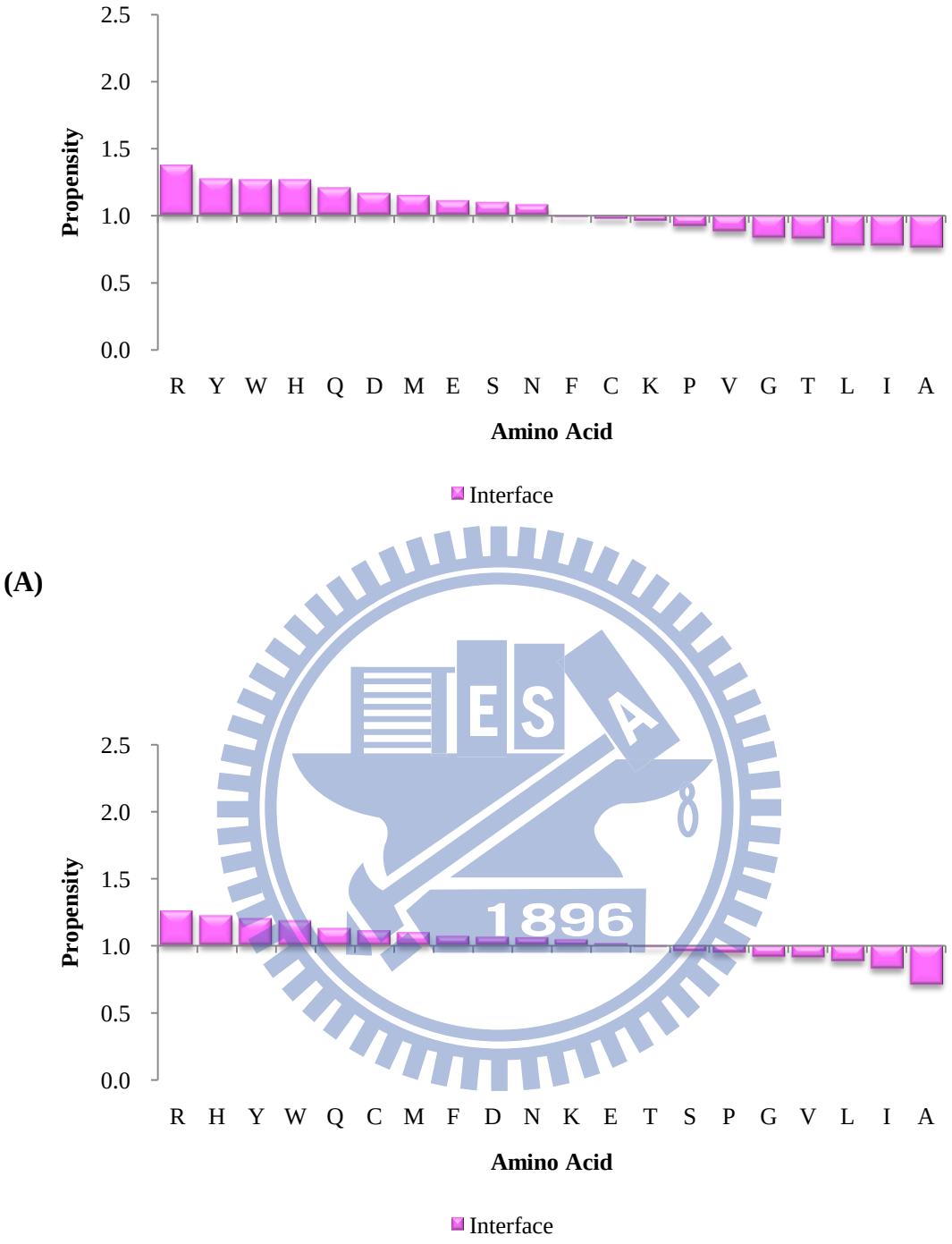

Figure 10. The amino acid propensities of interface in unbound state of (A) the ProMate database (B) the ZW database.

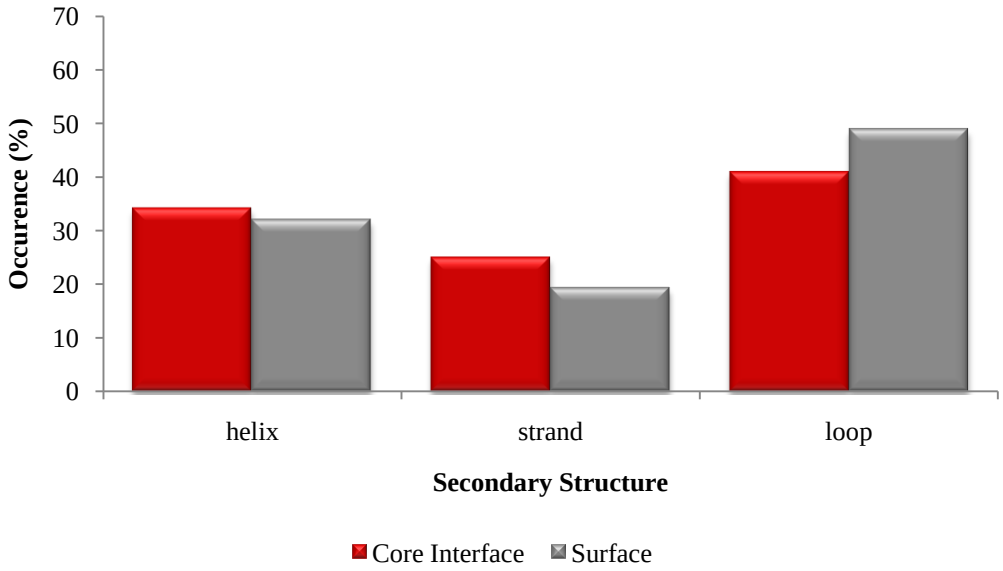

(A)

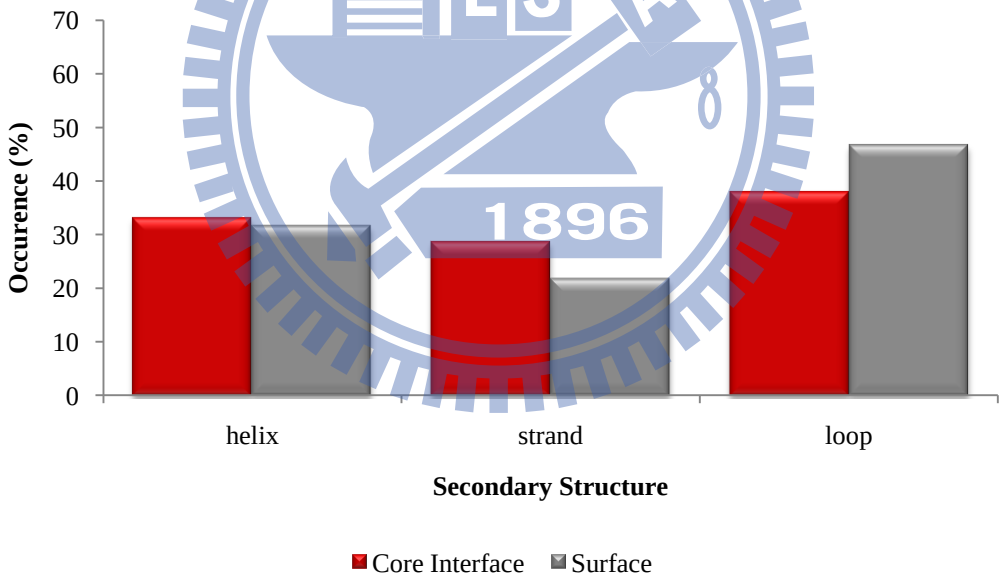

(B)

Figure 11. Comparison of the secondary structure distributions between core interfaces and surfaces in unbound state of (A) the ProMate database (B) the ZW database.

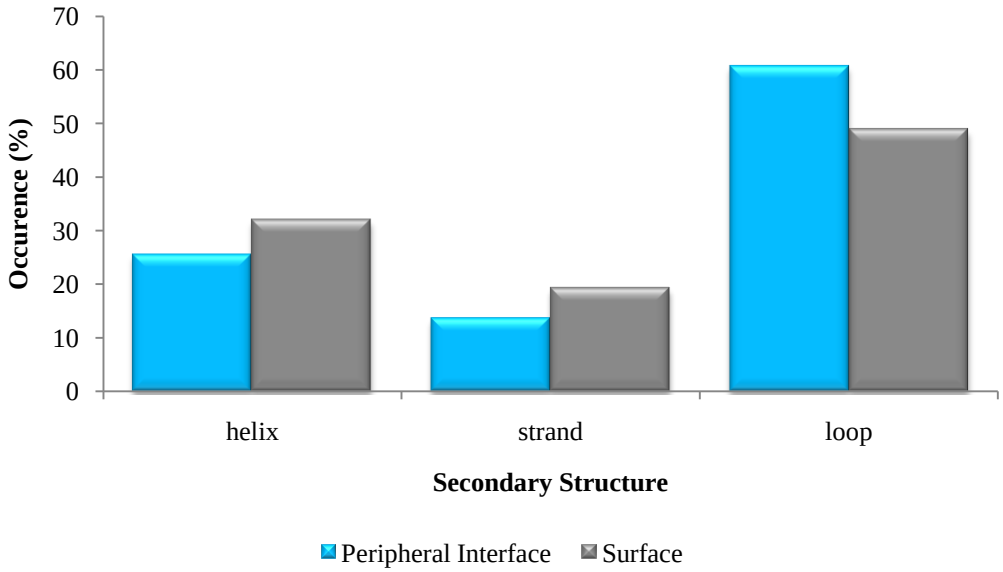

(A)

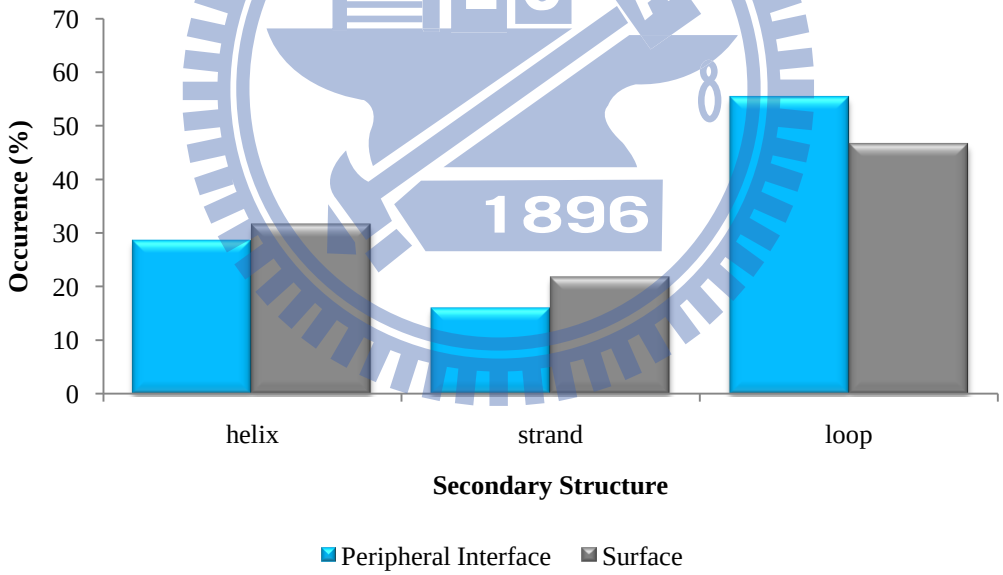

(B)

Figure 12. Comparison of the secondary structure distributions between peripheral interfaces and surfaces in unbound state of (A) the ProMate database (B) the ZW database.

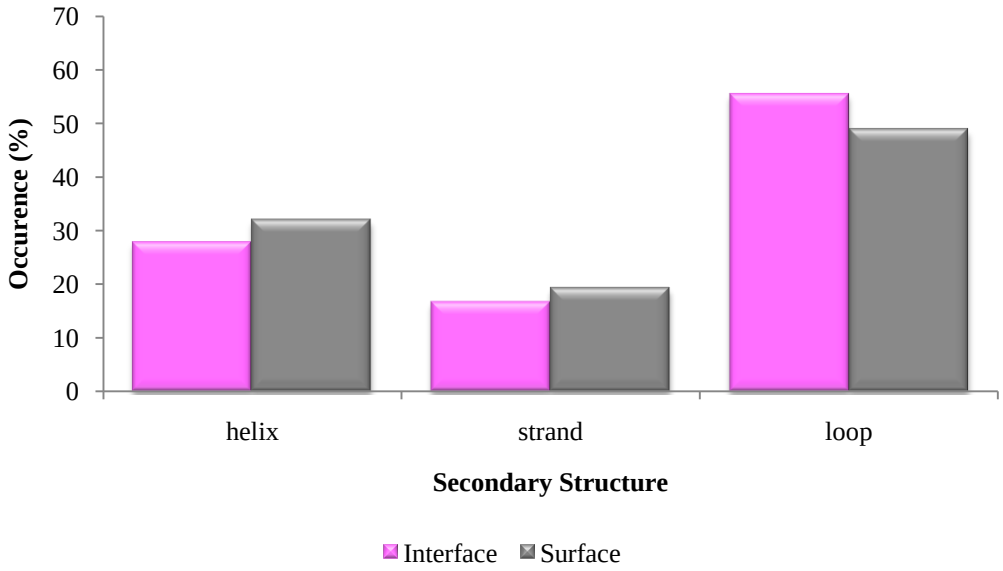

(A)

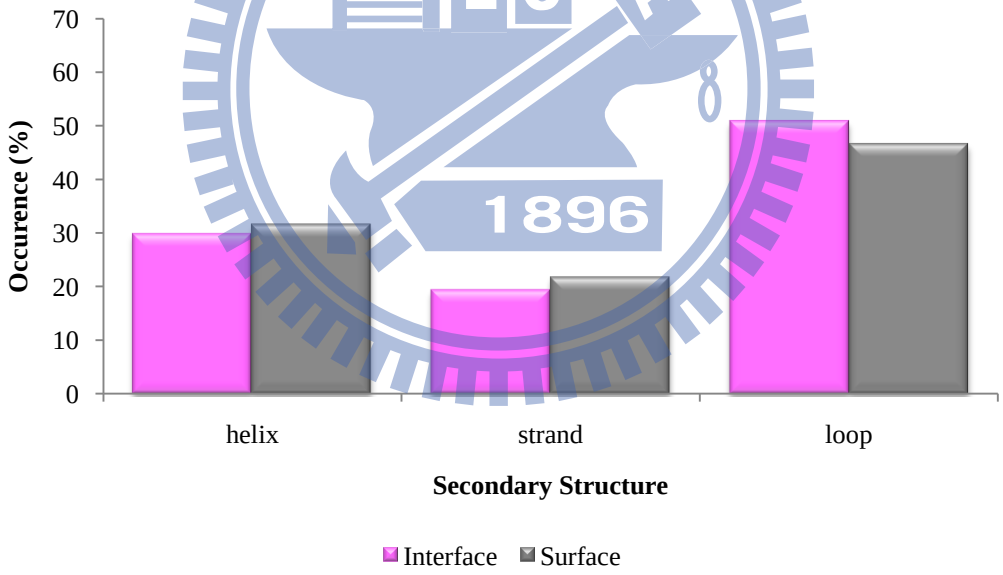

(B)

Figure 13. Comparison of the secondary structure distributions between interfaces and surfaces in unbound state of (A) the ProMate database (B) the ZW database.

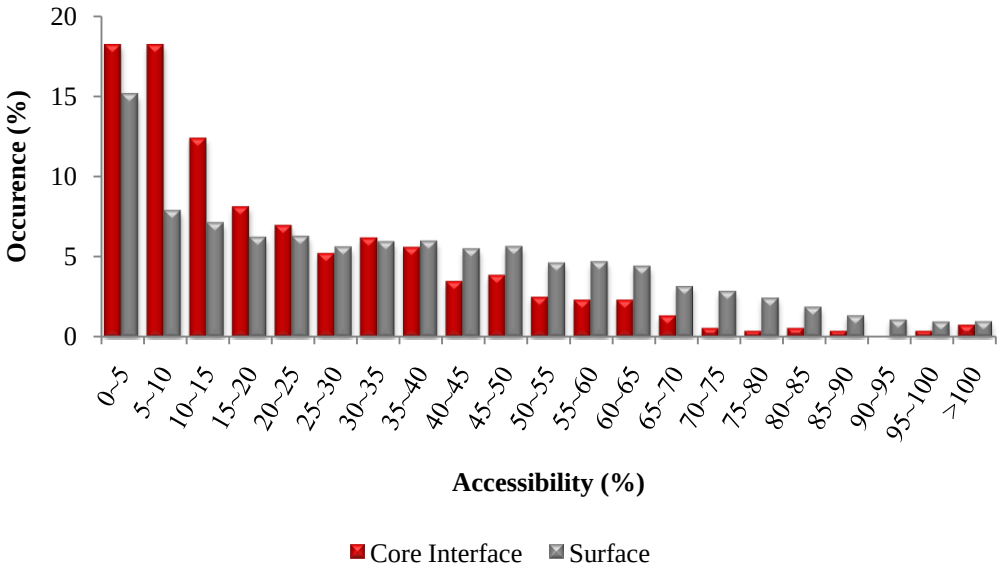

(A)

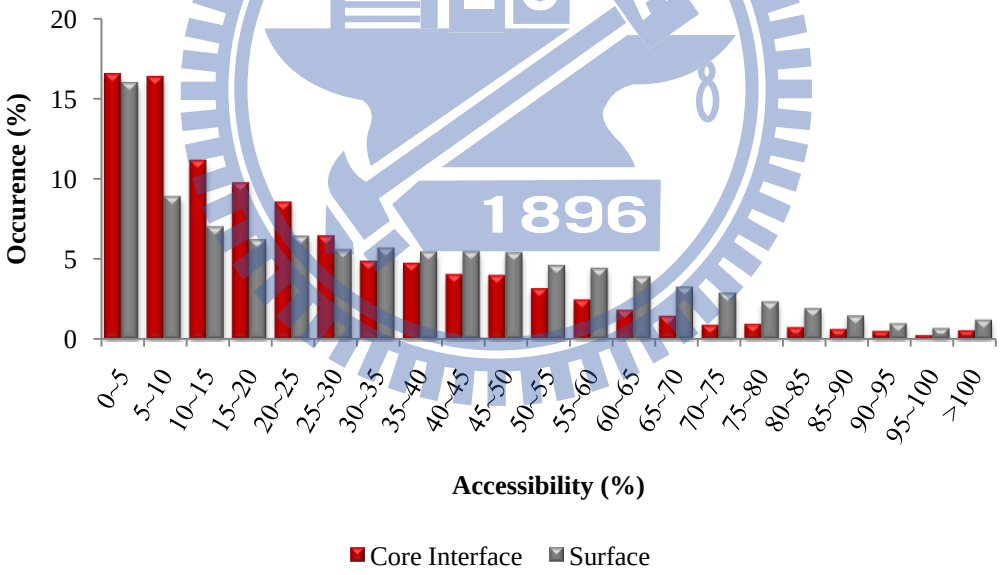

(B)

Figure 14. Comparison of the distributions of solvent accessibility between core interfaces and surfaces in unbound state of (A) the ProMate database (B) the ZW database.

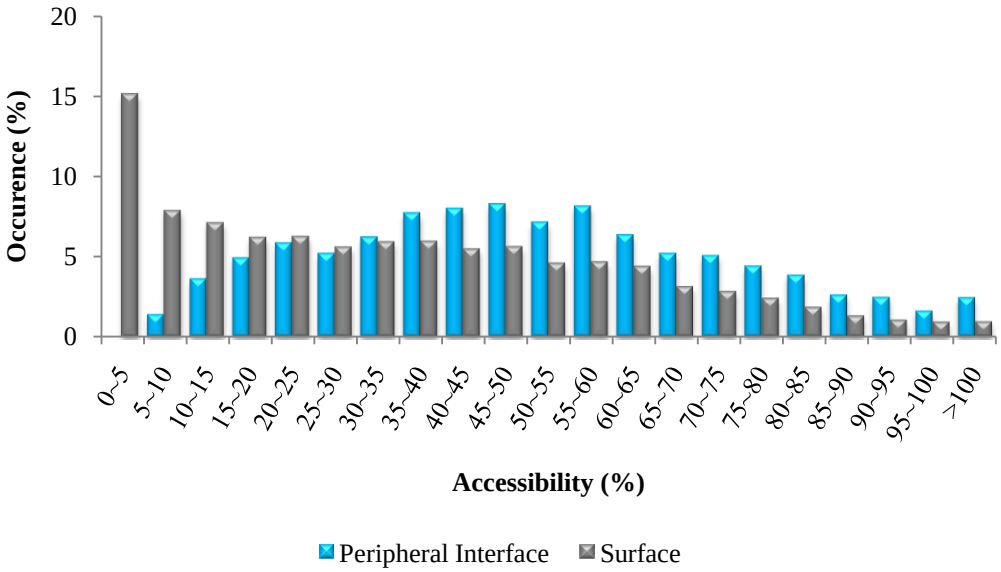

(A)

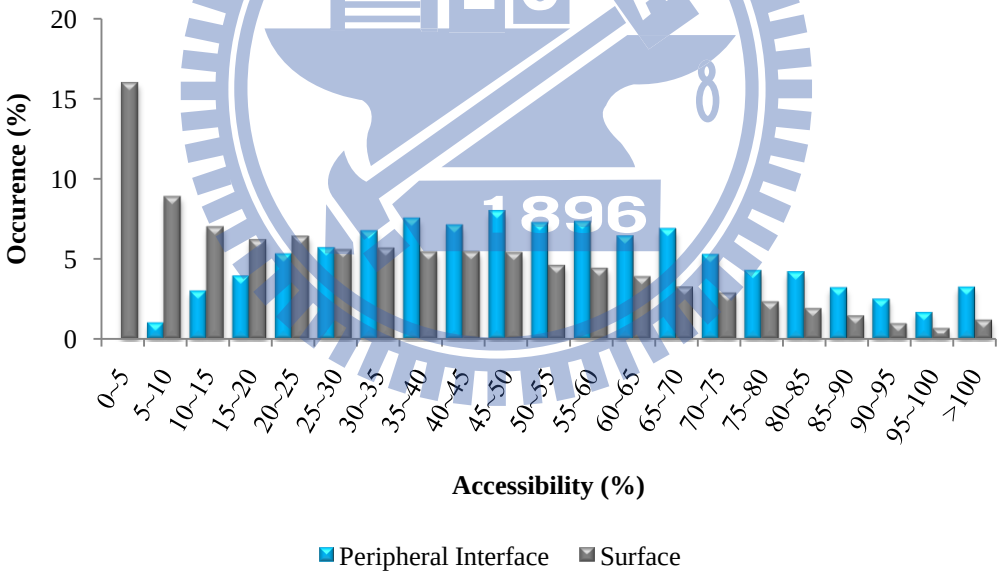

(B)

Figure 15. Comparison of the distributions of solvent accessibility between peripheral interfaces and surfaces in unbound state of (A) the ProMate database (B) the ZW database.

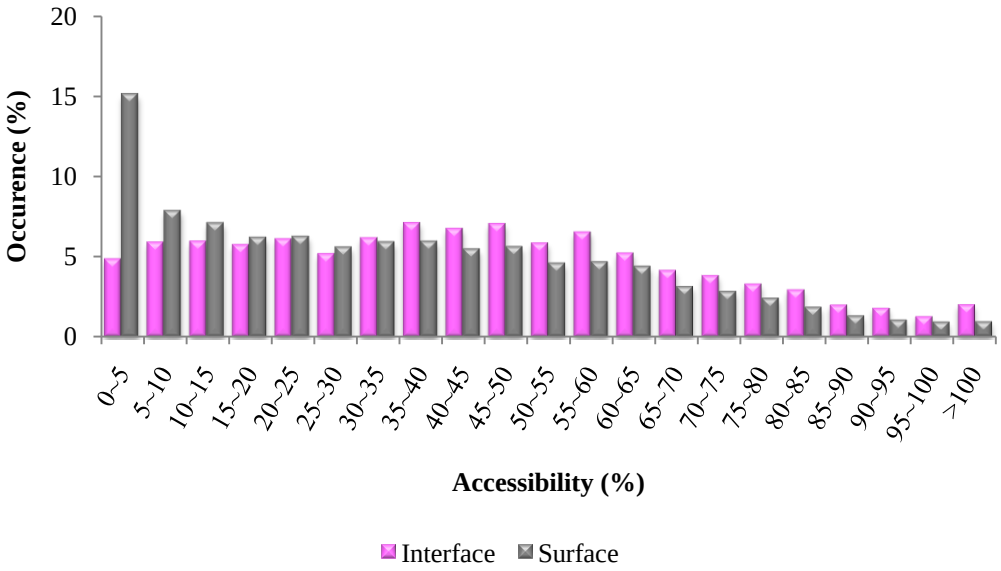

(A)

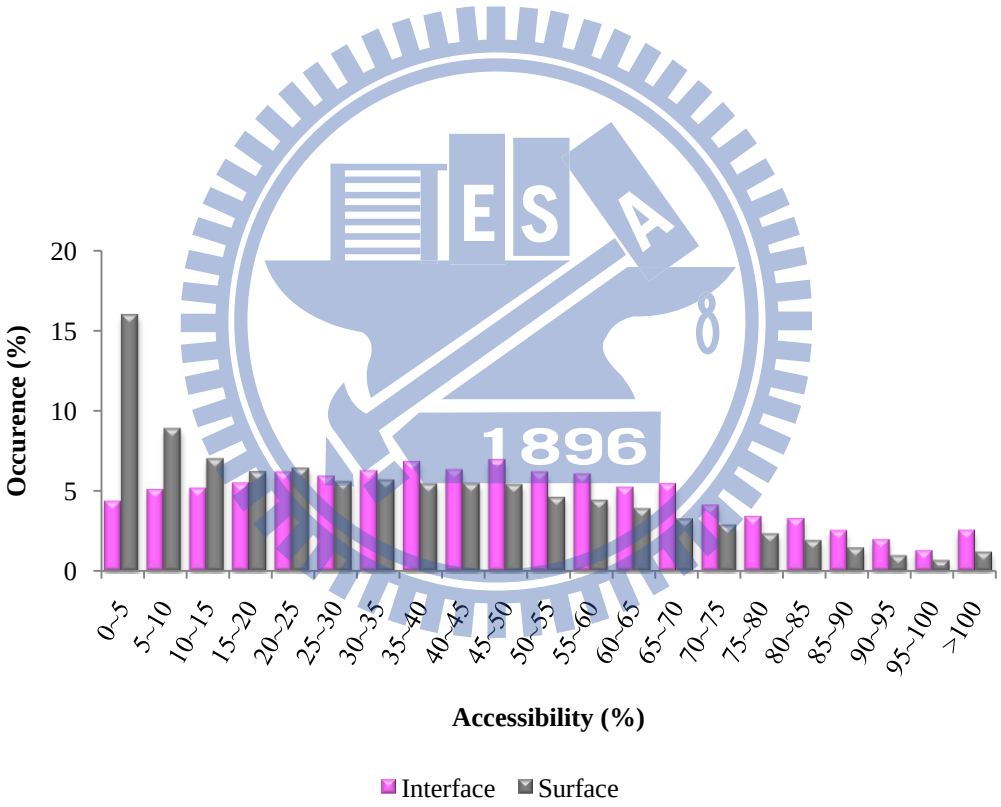

(B)

Figure 16. Comparison of the distributions of solvent accessibility between interfaces and surfaces in unbound state of (A) the ProMate database (B) the ZW database.

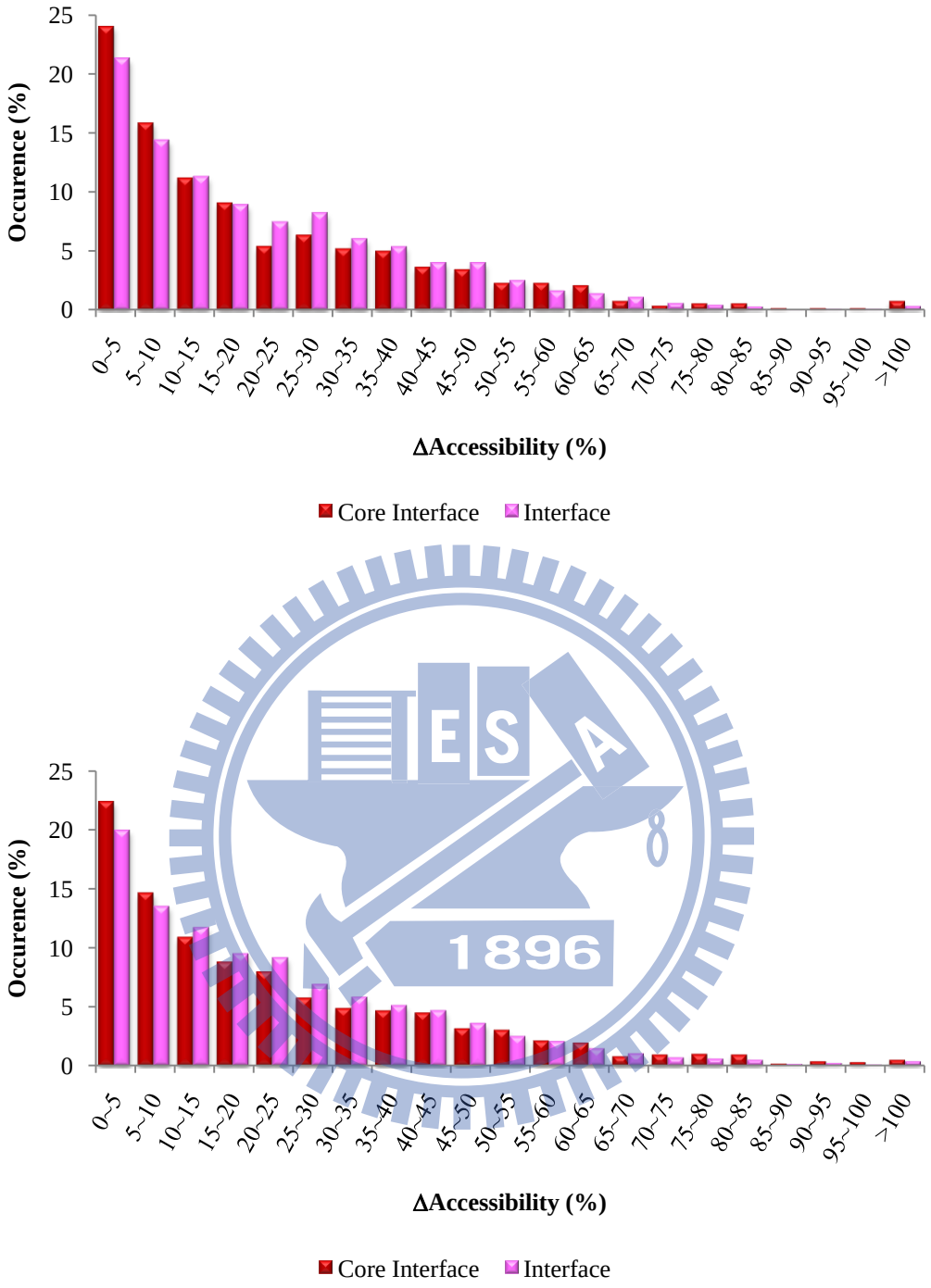

(A)

(B)

Figure 17. Comparison of the distributions of accessibility change between core interfaces and interfaces in complexation of (A) the ProMate database (B) the ZW database.

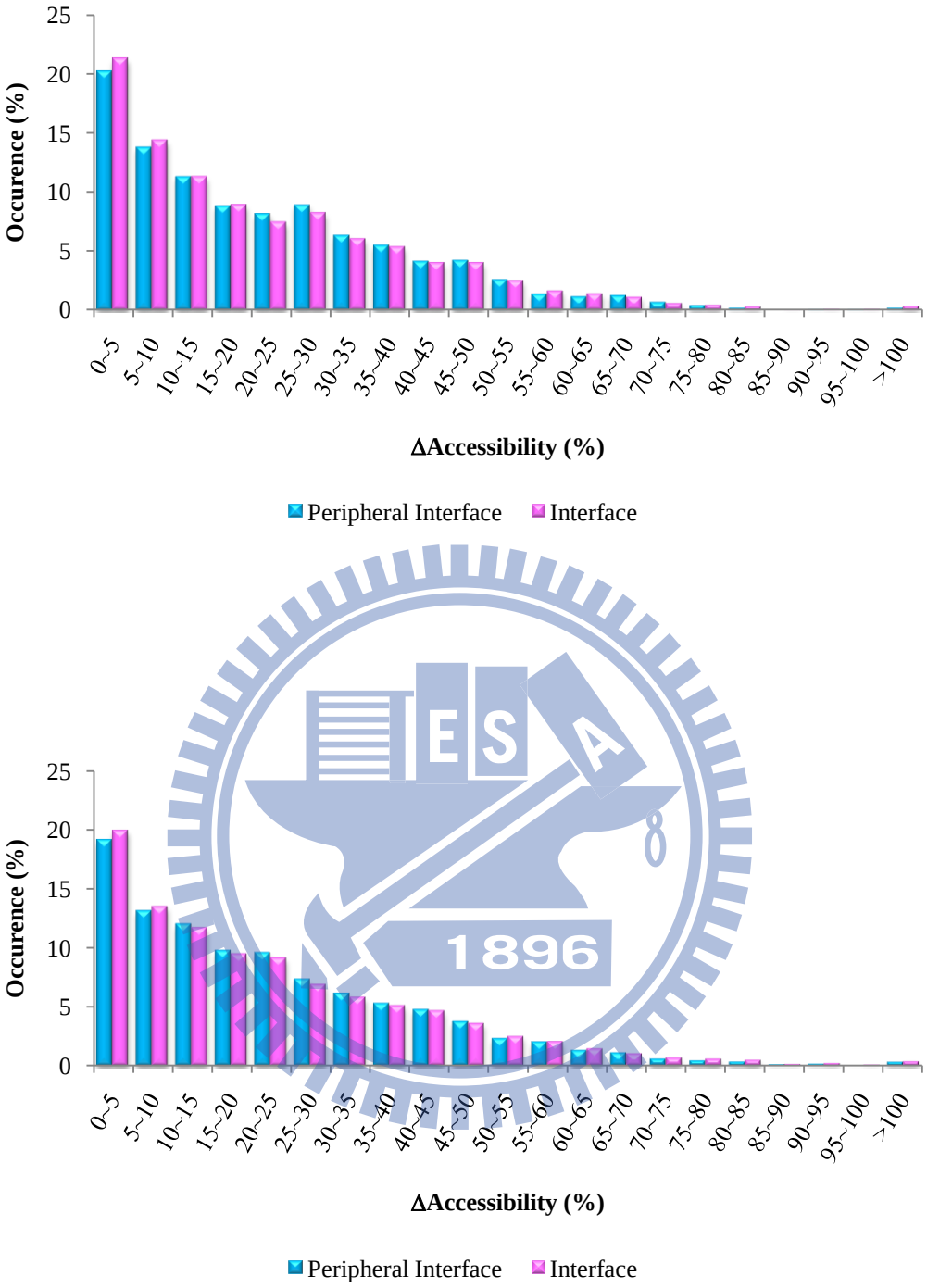

(A)

(B)

Figure 18. Comparison of the distributions of accessibility change between peripheral interfaces and interfaces in complexation of (A) the ProMate database (B) the ZW database.

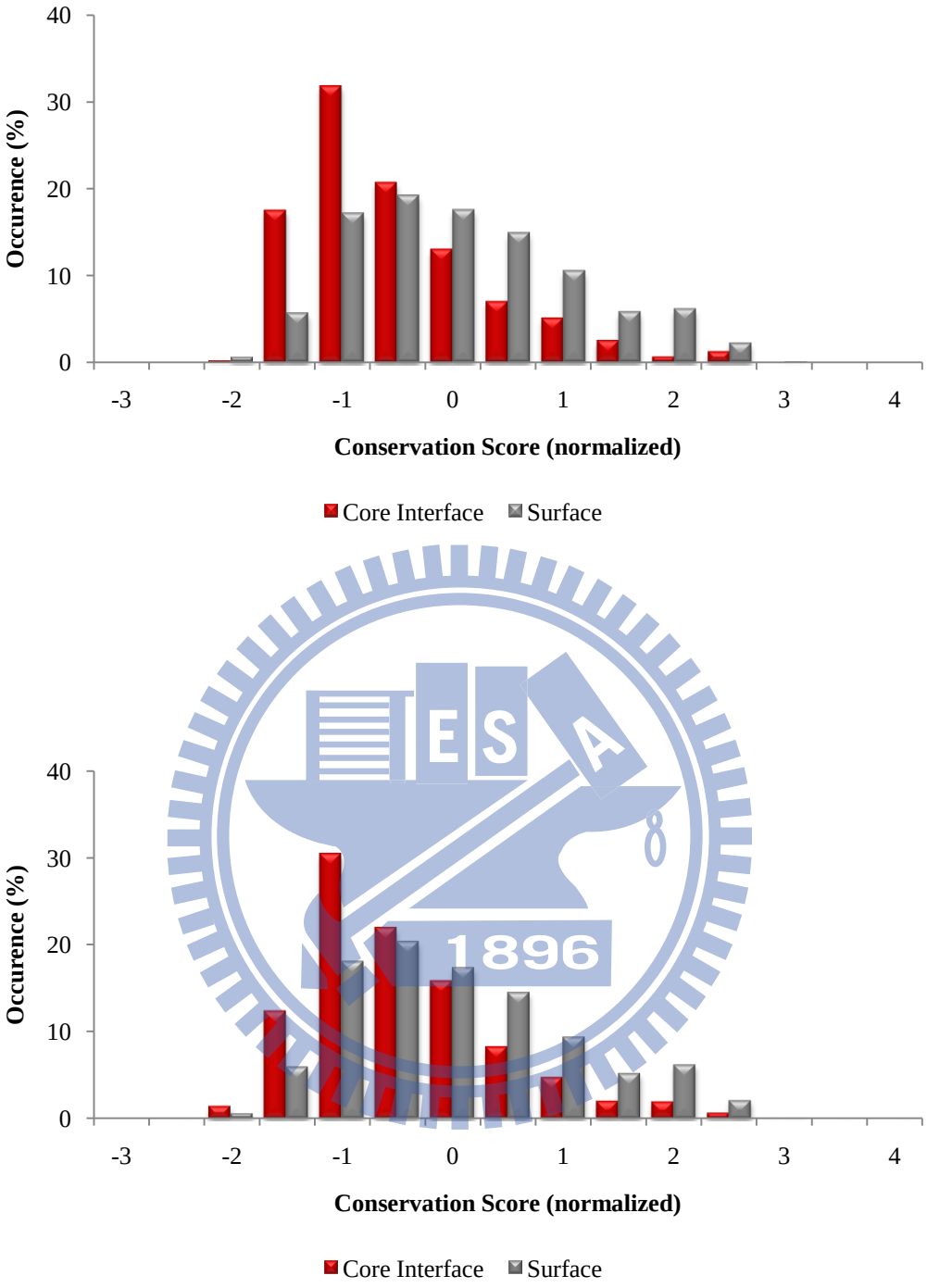

(A)

(B)

Figure 19. Comparison of the distributions of amino acid conservation scores between core interfaces and surfaces in unbound state of (A) the ProMate database (B) the ZW database.

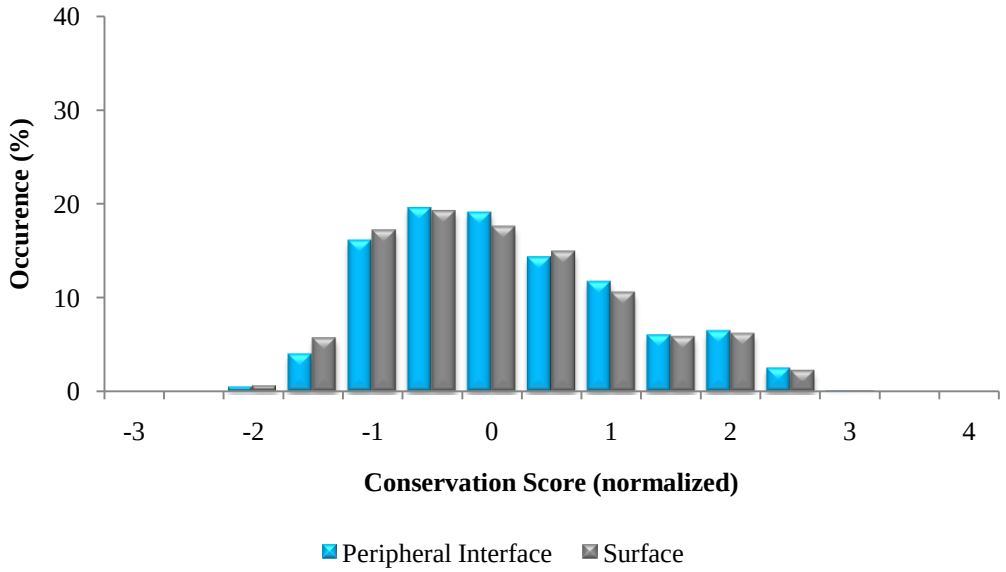

(A)

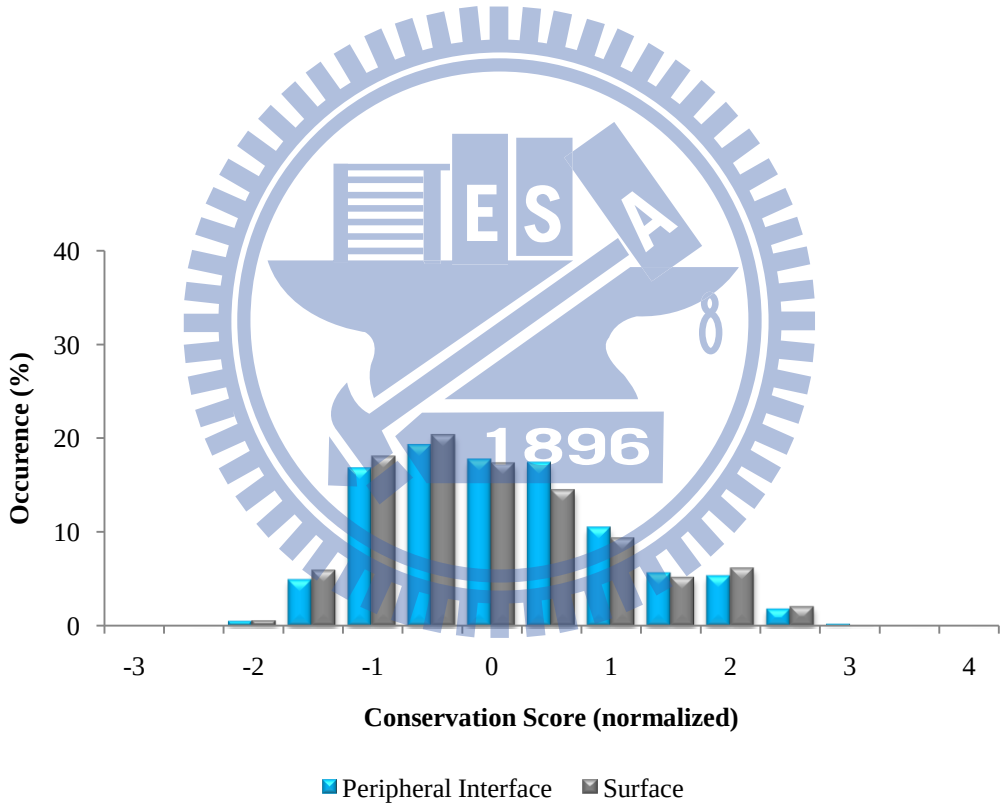

(B)

Figure 20. Comparison of the distributions of amino acid conservation scores between peripheral interfaces and surfaces in unbound state of (A) the ProMate database (B) the ZW database.

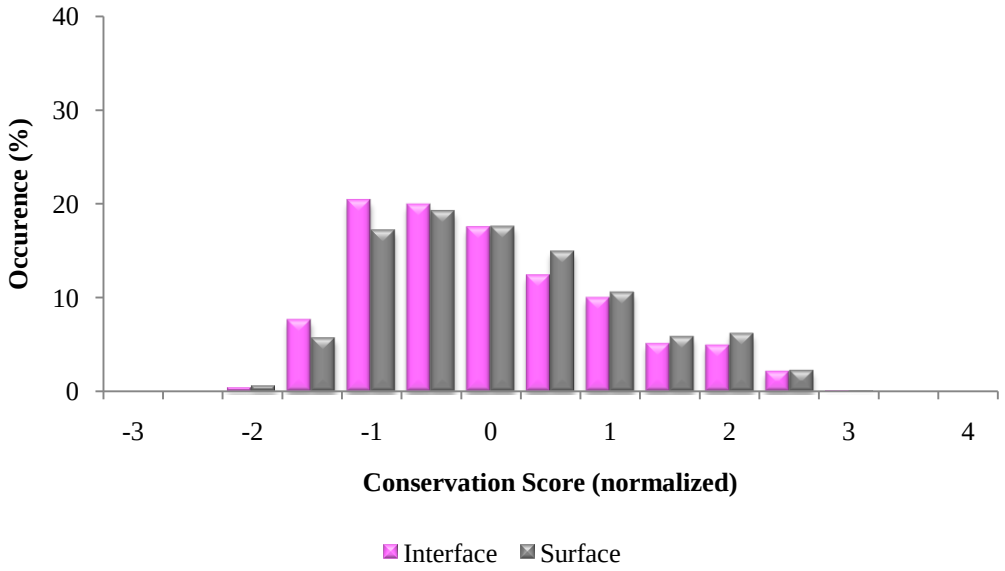

(A)

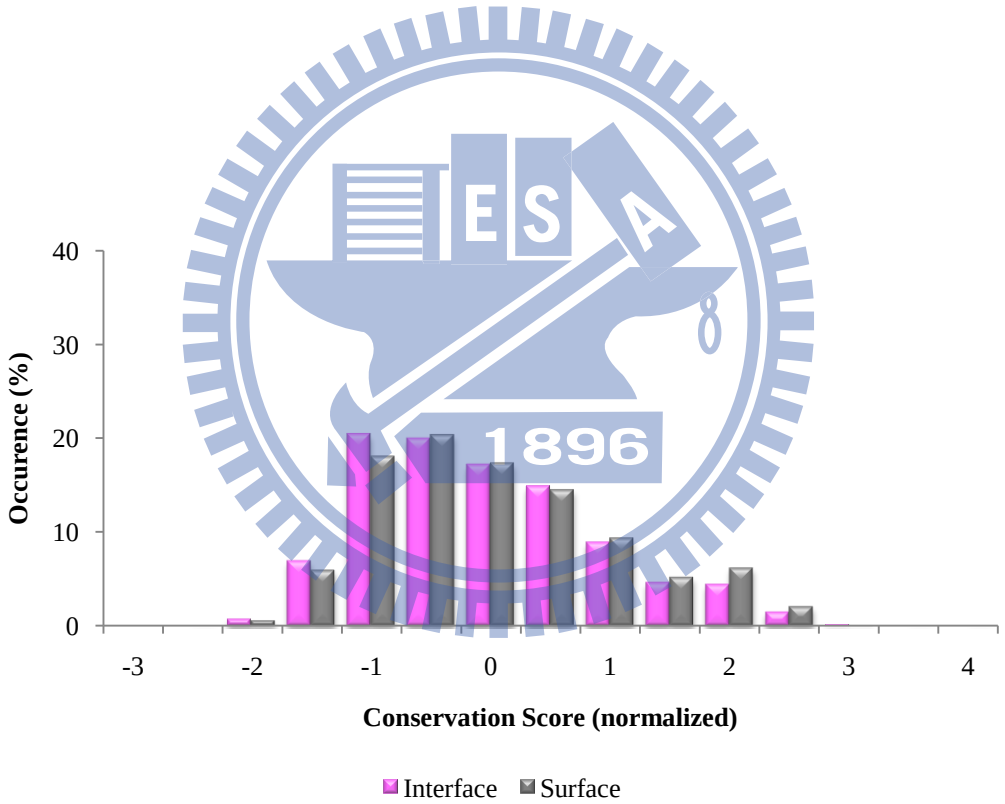

(B)

Figure 21. Comparison of the distributions of amino acid conservation scores between interfaces and surfaces in unbound state of (A) the ProMate database (B) the ZW database.

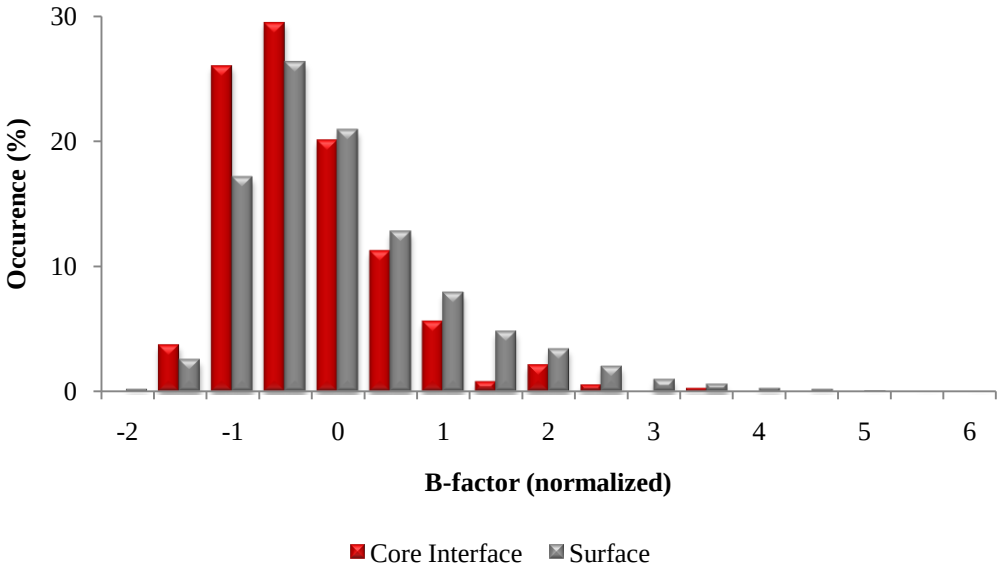

Figure 22. Comparison of the B-factor distributions between core interfaces and surfaces in unbound state of the ProMate database.

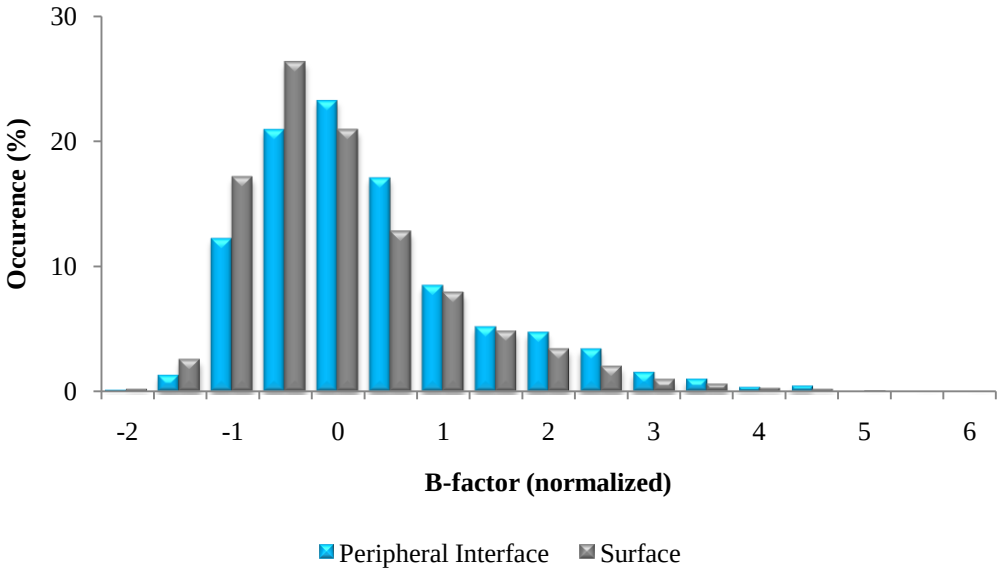

Figure 23. Comparison of the B-factor distributions between peripheral interfaces and surfaces in unbound state of the ProMate database.

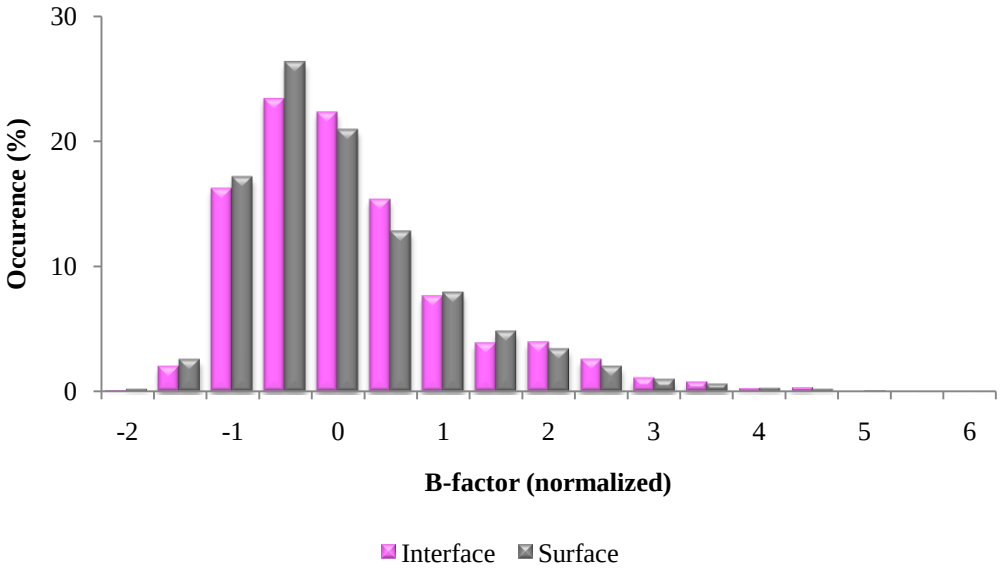

Figure 24. Comparison of the B-factor distributions between interfaces and surfaces in unbound state of the ProMate database.

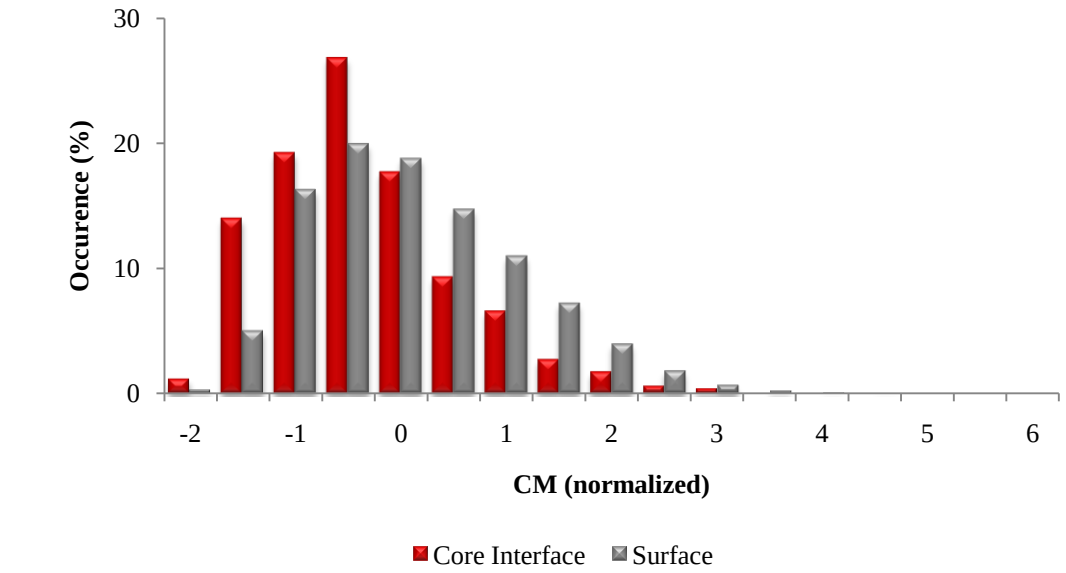

(A)

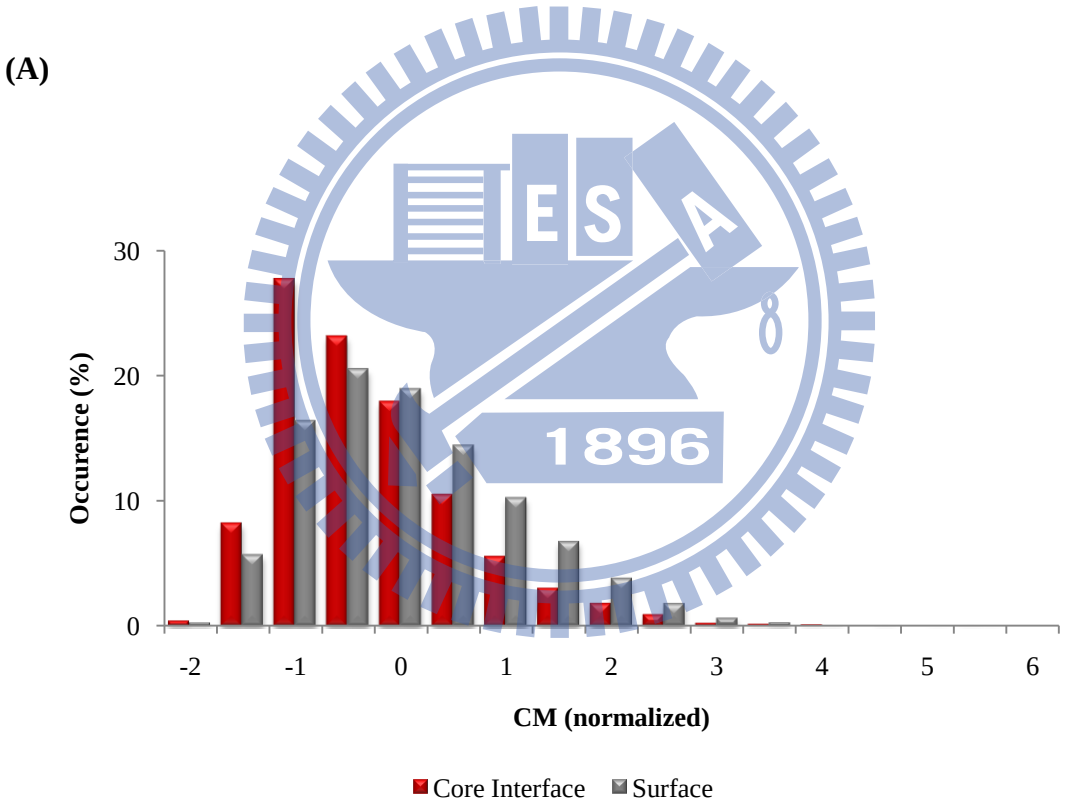

(B)

Figure 25. Comparison of the CM distributions between core interfaces and surfaces in unbound state of (A) the ProMate database (B) the ZW database.

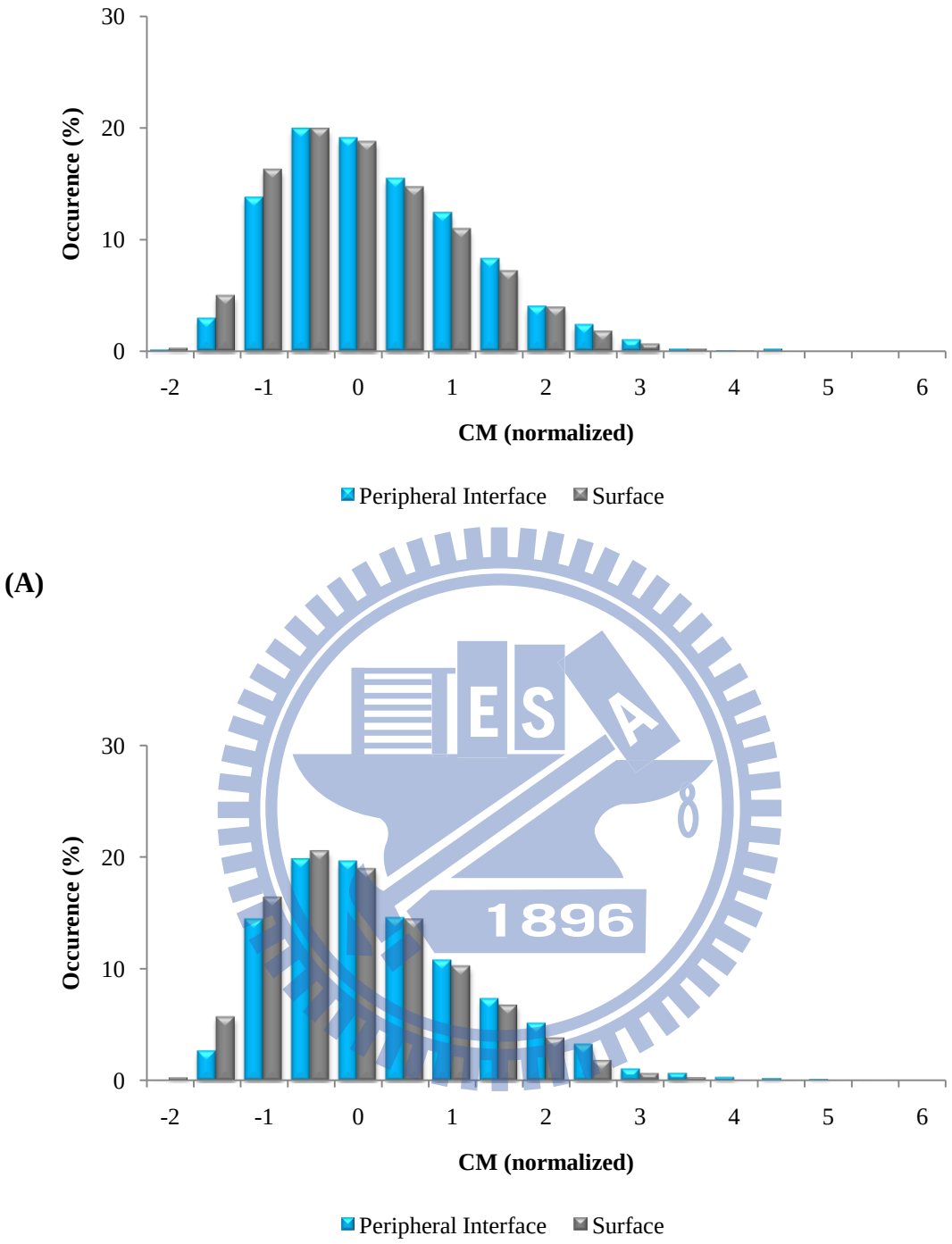

Figure 26. Comparison of the CM distributions between peripheral interfaces and surfaces in unbound state of (A) the ProMate database (B) the ZW database.

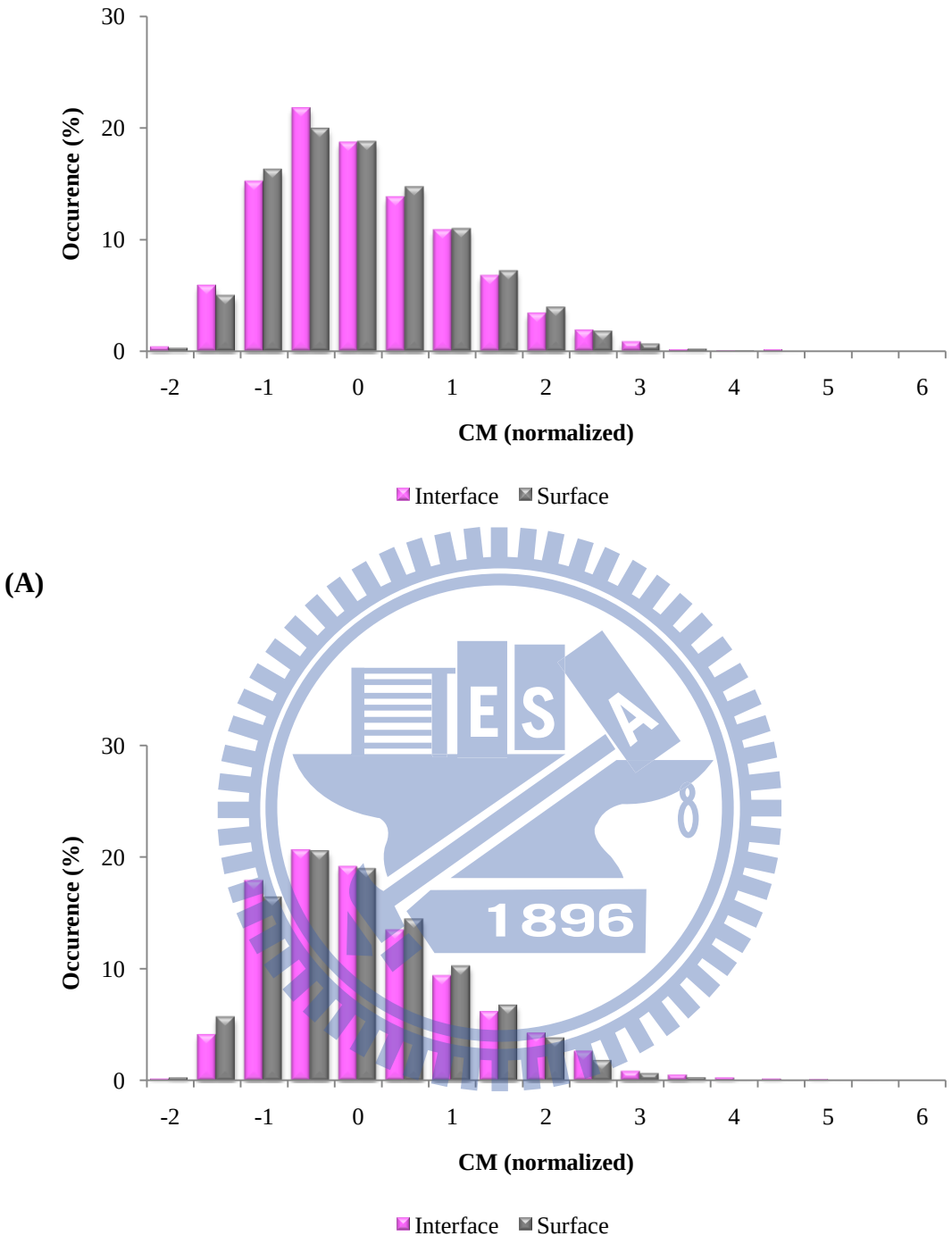

(A)

(B)

Figure 27. Comparison of the CM distributions between interfaces and surfaces in unbound state of (A) the ProMate database (B) the ZW database.

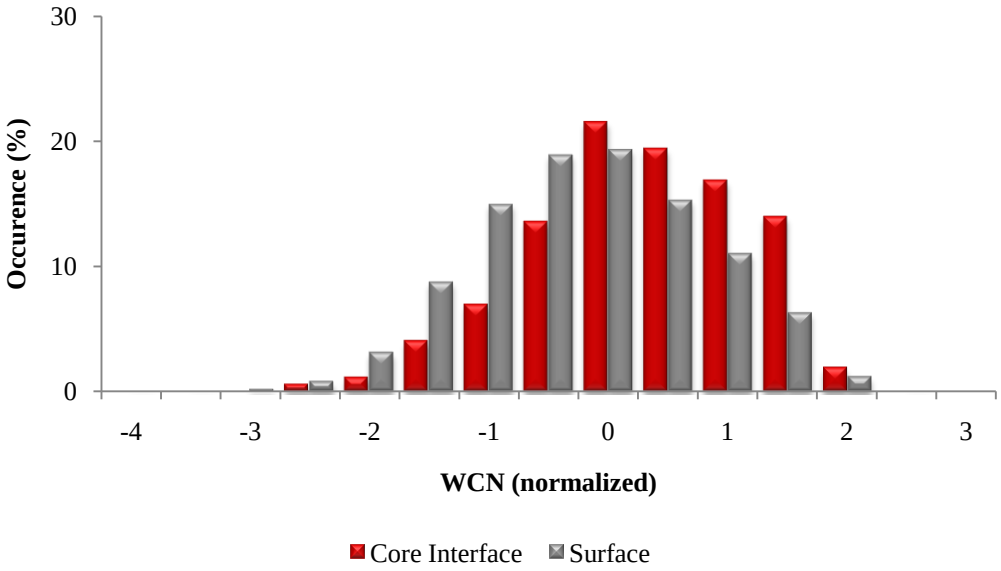

(A)

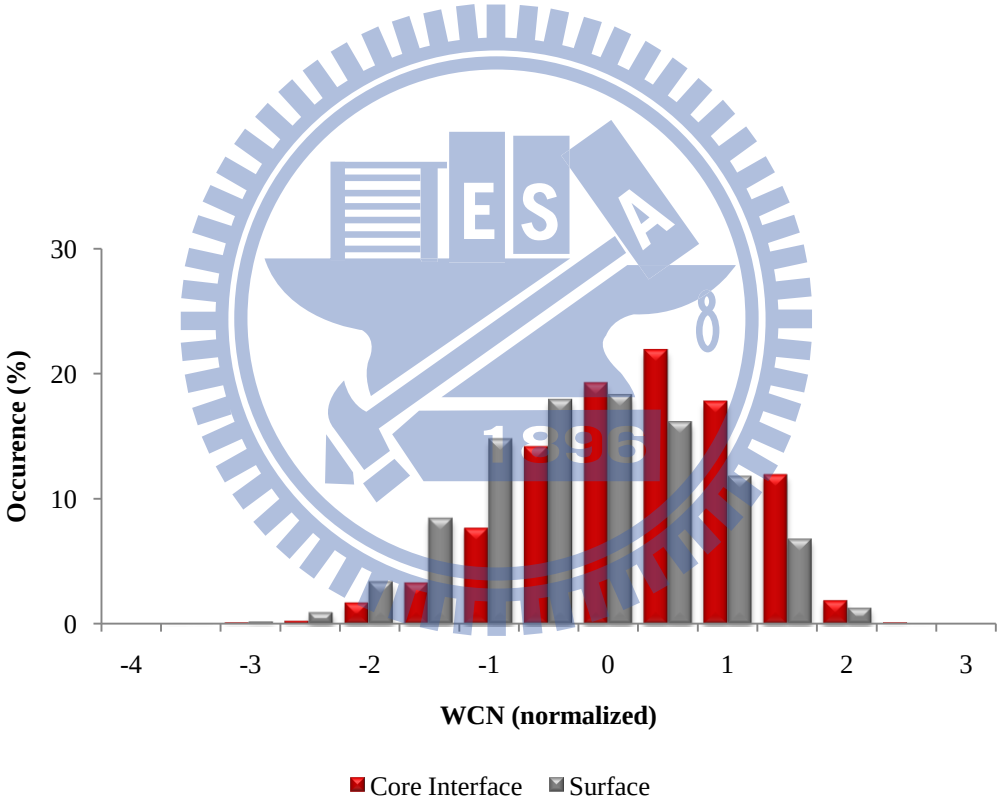

(B)

Figure 28. Comparison of the WCN distributions between core interfaces and surfaces in unbound state of (A) the ProMate database (B) the ZW database.

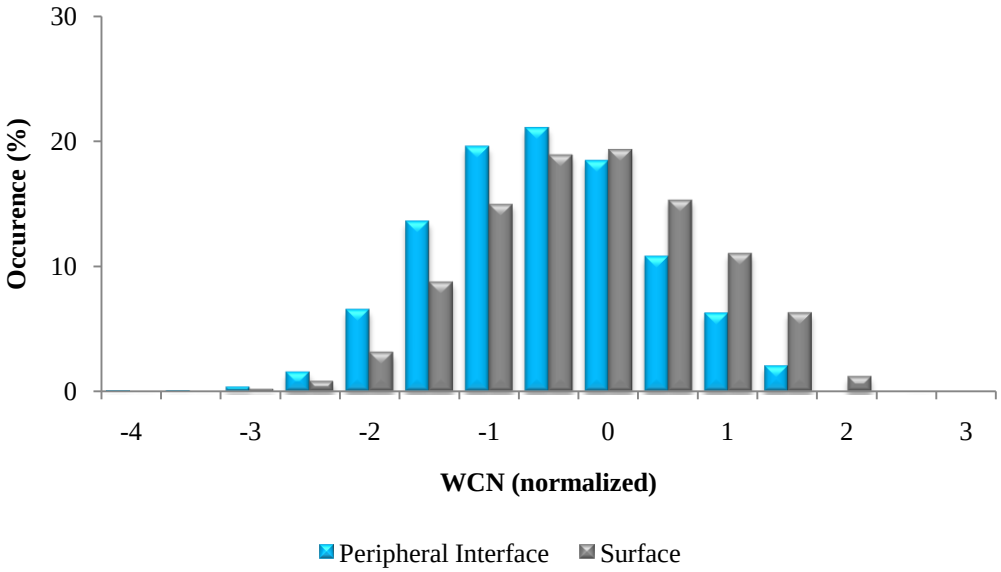

(A)

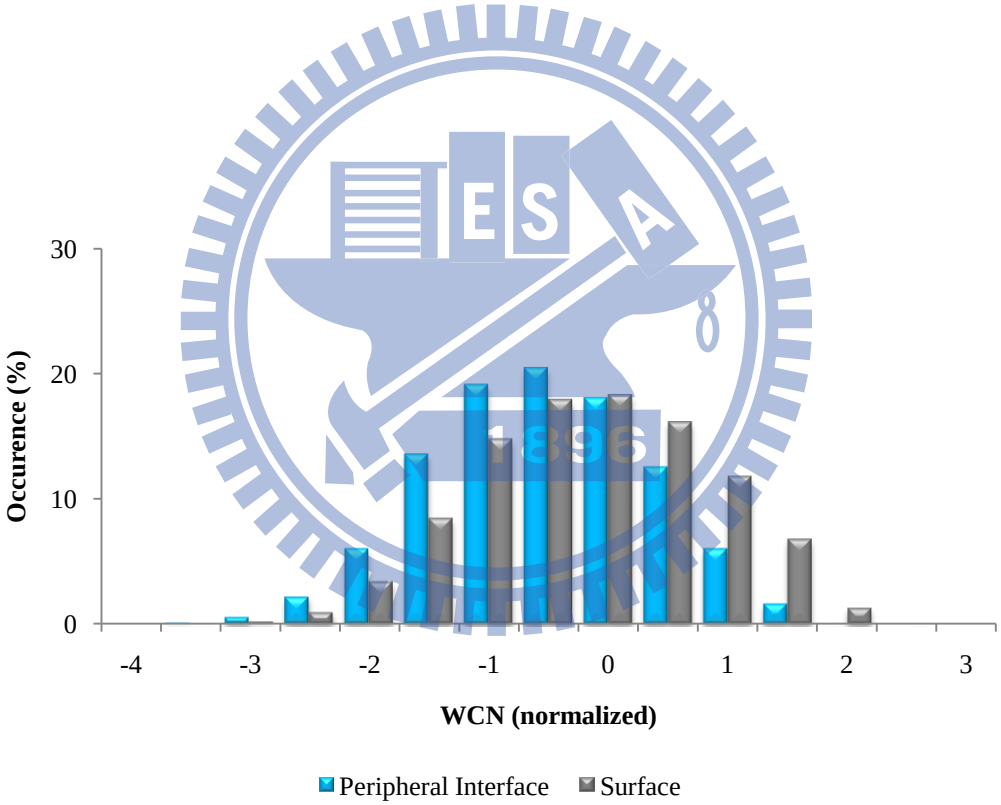

(B)

Figure 29. Comparison of the WCN distributions between peripheral interfaces and surfaces in unbound state of (A) the ProMate database (B) the ZW database.

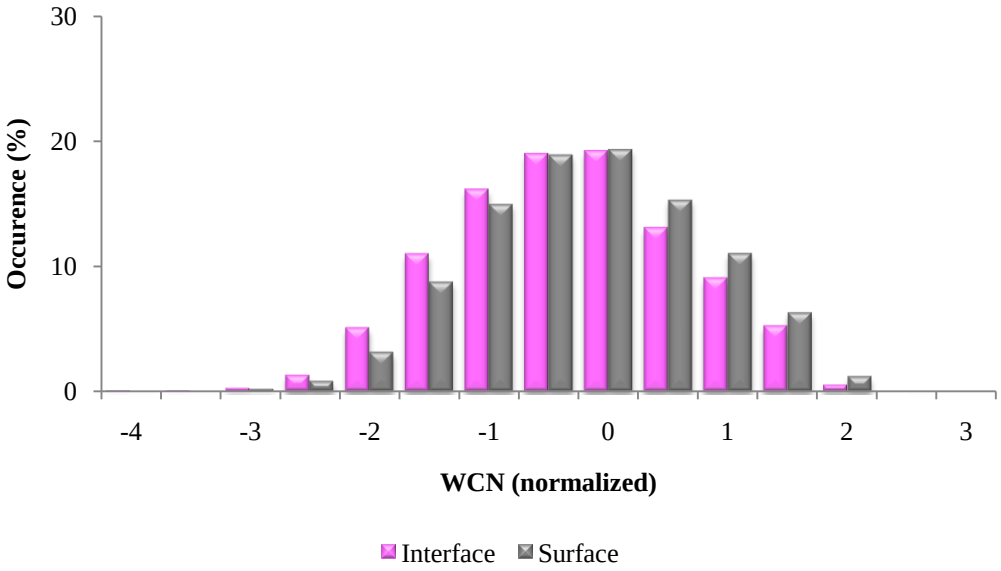

(A)

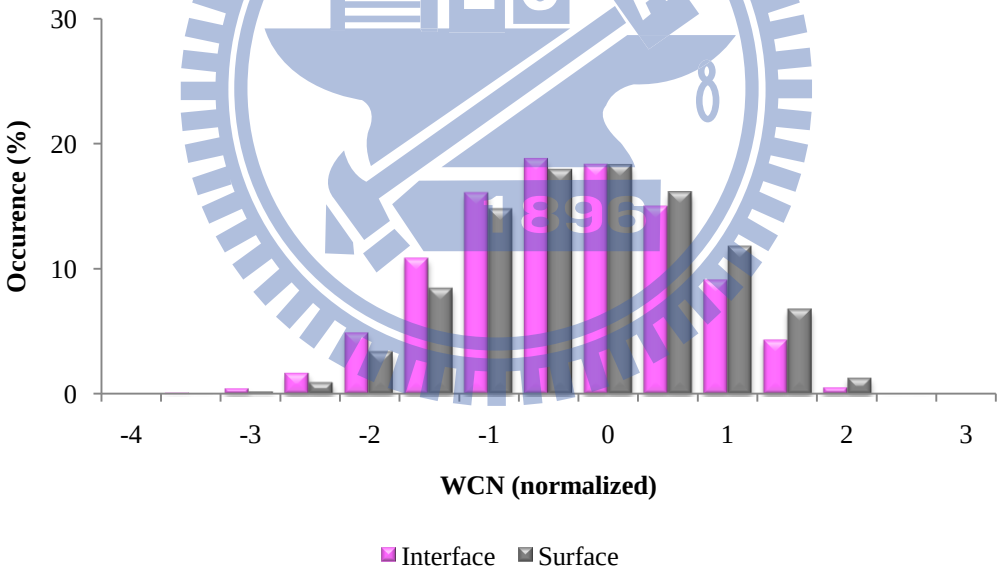

(B)

Figure 30. Comparison of the WCN distributions between interfaces and surfaces in unbound state of (A) the ProMate database (B) the ZW database.

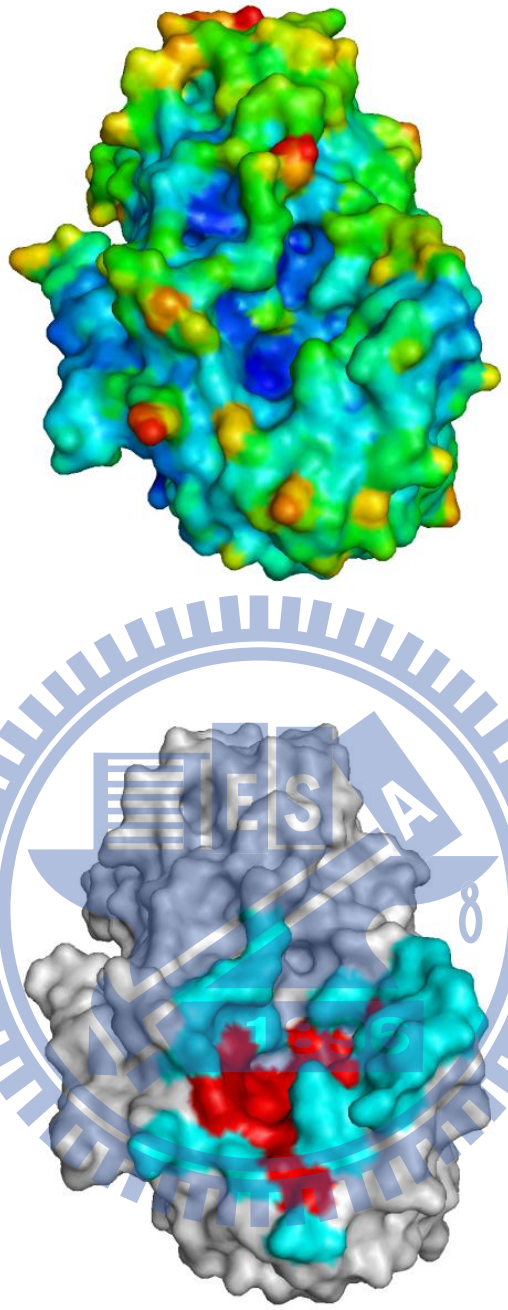

(A)

(B)

Figure 31. Visualization of the B-factor of the core interface and the peripheral interface (PDB entry 1tmq) (A) The chain A of 1tmq was colored by B-factors. (B) The chain A of 1tmq was colored in gray. The core interface and the peripheral interface were highlighted in red and cyan independently.

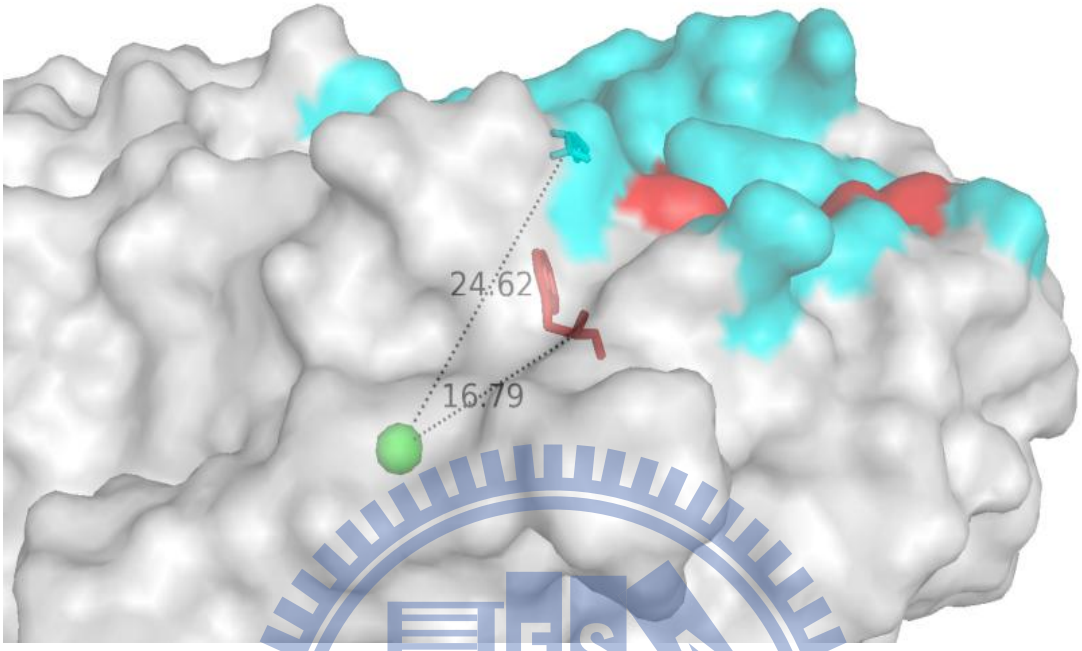

Figure 32. Visualization of the example of CM model (PDB entry: 1tmqA) The core interface and peripheral interface were shown as sticks and colored in red and cyan independently. The center of mass of chain A of 1tmq was pictured as sphere and colored in green. The distance of the core interface residue, W56, and the center of mass was 16.79 Å. The distance of the peripheral interface residue, E229, and the center of mass was 24.62 Å.

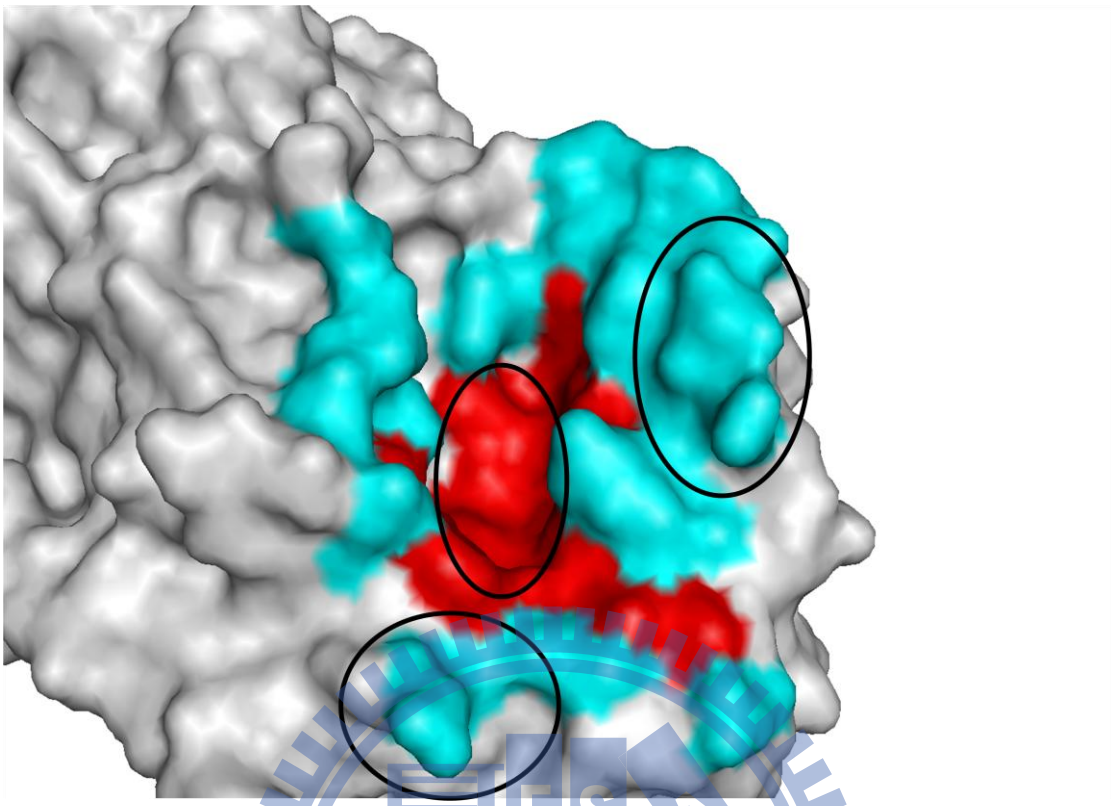

Figure 33. Visualization of the example of WCN (PDB entry: chain A of 1tmq)

Appendix

Homologous monomer	Equivalent bound		Homologous monomer	Equivalent bound		Homologous monomer	Equivalent bound
1a19A	1brsD		1eza_	3ezaA		1pne_	1hluP
1a2pA	1brsA		1eztA	1agrE		1poh_	1ggrB
1a5e_	1bi7B		1f00I	1f02I		1ppp_	1stfE
1acl_	1fssA		1f5wA	1kacB		1qqrA	1bmlC
1ag6_	2pcfA		1fkl_	1b6cA		1rgp_	1am4A
1aje_	1am4D		1flzA	1euiA		1selA	1cseE
1ajw_	1cc0E		1fvhA	1dn1A		1vin_	1finB
1aueA	1fapB		1g4kA	1ueaA		1wer_	1wq1G
1avu_	1avwB		1gc7A	1ef1A		1xpb_	1jtgA
1aye_	1dtdA		1gnc_	1cd9A		2bnh_	1a4yA
1b1eA	1a4yB		1hh8A	1e96B		2cpl_	1ak4A
1bip_	1tmqB		1hplA	1ethA		2f3gA	1ggrA
1ctm_	2pcfB		1hu8A	1ycsA		2nef_	1avzB
1cto_	1cd9B		1iob_	1itbA		2rgf_	1lfdA
1cye_	1eayA		1j6zA	1c0fA		3ssi_	2sicI
1d0nA	1c0fS		1jae_	1tmqA		6ccp_	2pcbA
1d2bA	1ueaB		1lba_	1aroL			1jtgB
1ekxA	1d09A		1nobA	1kacA			
1ex3A	1cgiE		1nos_	1nocA			
1ez3A	1dn1B		1pco_	1ethB			

Table1. List of proteins of ProMate database

2prg B:C	1ebd AB:C	1g0y I:R
1h59 A:B	1e6e A:B	1ijk A:BC
1c4z A:D	1gaq A:B	1n2c AB:EF
1evt A:C	1f80 A:E	1mah A:F
1dn1 A:B	1stf E:I	1gcq B:C
1xdt R:T	1f02 I:T	1www VW:X
1t7p A:B	2btc E:I	1i2m A:B
1go4 A:G	1gh6 A:B	1kgy A:E
1i85 B:D	1rlb ABCD:E	1c1y A:B
1jma A:B	1aro L:P	1gl4 A:B
1kac A:B	1ak4 A:D	1d2z A:B
1gc1 C:G	1i3o ABCD:E	3ygs C:P
1f51 AB:E	1atn A:D	1cs4 AB:C
1kmi Y:Z	1dkg AB:D	1efu A:B
7cei A:B	1b6c A:B	3sgb E:I
1bvn P:T	1qo0 A:DE	1fqv A:B
1qkz A:HL	1ugh E:I	1k3z AB:D
1dpj A:B	1df9 B:C	1m4u A:L
1f83 A:BC	1jiw I:P	1m2o AC:B
1fak HL:T	1f93 AB:EF	1mbu A:C
1jw9 B:D	1noc A:B	1fc2 C:D
1jtd A:B	1hwg A:BC	1ml0 A:D
1d5x A:C	1fg9 AB:C	1gvn AC:B
1i4e A:B	1ebp A:CD	1o6s A:B
1ib1 AB:E	1du3 A:DEF	1h2k A:S
2pcc A:B	1euv A:B	1m1e A:B
1f3v A:B	1de4 CF:A	1o94 AB:CD
1lpb A:B	1ghq A:B	1nf5 A:B
1ay7 A:B	1flt VW:X	1gzs A:B
1kkl ABC:H	1gxd A:C	1nbf A:D
1dev A:B	1ycs A:B	1mr1 A:D
1l0o AB:C	1gla F:G	
1dfj E:I	2sic E:I	
1g4y B:R	1jsu AB:C	
1jch A:B	1is8 ABEJCIDHGF:KLOMN	

Table2. List of proteins of ZW database